Steering Adaptation: Firm, Labor Contracts, and Driver Responses to Heat in the Trucking Industry

Wenzhi Dave Ding[*] Xincheng Wang[†]
Yucheng Wang[‡] Zhenxuan Wang[§]

This draft: March. 2026

[Preliminary. Please Do Not Circulate.]

Abstract

We study how firms shape workers' adaptation to climate risk. Using real-time GPS and driver-monitoring data on 10,000 truck drivers over 15 months, we show that exposure to extreme heat worsens driver performance and induces adaptive responses. Firms play a central role in shaping both adaptation choices and their consequences. Relative to employee drivers, owner-operators are less likely to use air conditioning and instead adapt by taking more rest and adjusting their labor supply. Firms also mitigate negative productivity shocks by dispatching additional trucks on hot days. As a result, the adverse effects of heat are about twice as large for owner-operators as for employee drivers. To rationalize the observed heterogeneous adaptation, we develop and quantify a model in which firms share adaptation costs and steer workers' behavior, trading off the benefits of adaptation against moral hazard.

Keywords: Extreme Heat, Adaptation, Asset Ownership, Trucking, Moral Hazard
JEL: R40, R41, Q51, Q54, J28

[*]The Hong Kong Polytechnic University. Email: wenzhi.ding@polyu.edu.hk.
[†]The University of Hong Kong. Email: xcwang@hku.hk.
[‡]School of Economics, University of Sydney. Email: yuchengwangecon@gmail.com.
[§]Department of Agricultural and Resource Economics, North Carolina State University. Email: zhenxuan.wang@ncsu.edu.

1 Introduction

As global warming increases workers' exposure to high ambient temperatures, heat-related workplace injuries and economic losses are becoming an increasingly important policy concern.[1] However, the impact of heat depends not only on exposure itself but also on how workers and firms adapt to mitigate its harms. Workers can respond along several margins, such as taking more frequent breaks, increasing air conditioning usage, or adjusting work schedules, but these responses often come with a cost. When workers bear adaptation costs privately, adaptation may be inefficiently low because some of the benefits spill over beyond the individual worker. Conversely, when firms fully cover these costs, workers may overuse adaptation, giving rise to moral hazard. This incentive misalignment makes employer policies and labor contracts central to understanding adaptation behavior.

Despite growing policy attention to workplace protections against extreme heat, evidence remains limited on how workers adapt to high temperatures and how firms shape these responses. A key challenge is that, when researchers observe only aggregated outcomes, adaptation behaviors are difficult to distinguish from the direct effects of temperature, and firms' responses are difficult to disentangle from drivers' realized outcomes.[2]

This paper addresses these challenges by utilizing driver monitoring sensor data and unique empirical settings from the heavy-duty truck industry in China. The data includes real-time GPS records and AI-enhanced monitoring of the driving cabin. These data allow us to separately measure direct performance consequences (such as fatigue, distraction, lane departures, and collision risks) and adaptation behaviors (such as air conditioning usage, rest-taking, and changes in work schedules). Importantly, our setting features two distinct labor contracts: drivers either operate as independent owner-operators affiliated with a freight company or work as employees. This institutional variation shifts both the incidence of adaptation costs and the nature of incentive distortions. Owner-operators

[1] A growing body of evidence shows that extreme temperatures significantly impair labor performance, leading to increased work-related illnesses (Ireland, Johnston and Knott, 2023), higher rates of workplace accidents (Park, Pankratz and Behrer, 2021; Filomena and Picchio, 2024; Drescher and Janzen, 2025), and declines in productivity or labor supply (Graff Zivin and Neidell, 2014; Somanathan et al., 2021). The economic consequences can be substantial, particularly in labor-intensive sectors and occupations involving outdoor work (Zhang et al., 2018; Rode et al., 2022).

[2] For example, in the context of road transportation, most prior studies rely on traffic crash or fatality statistics as outcomes, which reflect a combination of both direct effects and adaptation behaviors. Furthermore, these variables are typically measured at a relatively low frequency (e.g., annual or monthly level), which exacerbates the problem, as they may be confounded with other factors such as changing road conditions or traffic volume during heat waves (Leard and Roth, 2019).

bear operating costs directly and choose adaptation based on their perceived heat damages and private benefits. Firms, by contrast, share part of these costs for employee drivers, but in doing so face the risk of moral hazard from excessive adaptation.

The heavy-duty trucking industry provides an attractive setting for our analysis. Truck drivers are often exposed to heat in confined and poorly ventilated environments, making heat exposure especially salient. The industry also features clearly defined tasks and objective measures of performance, allowing us to observe behavior and outcomes with unusual precision. Importantly, it presents a classic make-versus-buy distinction in labor organization, between owner-operators and company-employed drivers, which allows us to study how contract form shapes climate adaptation. Because similar contractual arrangements are widely used beyond trucking, the implications of our setting extend more broadly to how labor contract form shapes adaptation to climate risk across sectors.[3]

We compile a panel dataset that combines high-frequency driver-monitoring data with satellite weather imagery to track drivers' heat exposure, performance outcomes, and adaptation behaviors.[4] To estimate the effects of heat exposure, we exploit variation in drivers' exposure to the daily distribution of hourly temperatures. We control for a rich set of spatial factors, such as topography, and control for traffic conditions using speedometer readings. We also include driver-by-vehicle and date fixed effects to absorb unobserved factors such as driver experience, vehicle quality, and time-varying shocks other than weather. To address the concern that drivers may endogenously adjust routes and work schedules in response to heat, thereby contaminating our heat exposure measures, we construct an alternative heat exposure measure based on template-predicted routes and schedules as a robustness check.

We begin our analysis by first establishing that extreme heat is a negative shock to driver performance. Higher temperatures increase the incidence of dangerous driving behaviors: an additional hour of exposure to temperatures above 33°C raises dangerous driving incidents by 3% for the average driver. Extrapolated to the population of truck drivers in China, this effect implies annual economic losses of $281 million. Extreme heat also reduces productivity by lowering total daily working time and delivery distance.

Second, we turn to how drivers respond to this negative shock. We document both short-run behavioral adjustments and longer-run acclimatization. In the short run, drivers

[3]For example, Dey and Houseman (2025) show that contract workers accounted for about 10 percent of core manufacturing occupations in the United States, and that their prevalence has been rising over time.

[4]The high temporal frequency and fine spatial granularity of our data address common measurement issues in temperature exposure typically encountered when using pre-aggregated data over large regions or infrequent time intervals (Ghanem and Smith, 2021; Cui et al., 2024).

respond to heat stress by increasing air conditioning usage, taking more frequent and longer rests, and adjusting their labor supply and work start times. Over time, drivers with greater cumulative exposure to high temperatures and more driving experience exhibit fewer heat-induced dangerous driving behaviors, consistent with improved adaptation to extreme conditions.

Third, we find substantial heterogeneity in adaptation choices across labor contracts. Given the same menu of available adaptation margins, owner-operators are more likely to respond by increasing rest and adjusting their work schedules. Employee drivers, by contrast, respond primarily through greater air conditioning usage and are much less likely to adapt by resting or changing their labor supply. As a result, the adverse effects of heat are about twice as large for owner-operators as for employee drivers. In addition, we find that individual-level productivity losses do not fully pass through to firm-level losses in delivery loads or total miles driven, as firms mitigate these shocks by dispatching additional drivers on hot days.

Taken together, our empirical findings suggest that workers do respond to heat shocks, but firms and labor contracts play a central role in shaping both adaptation behavior and its consequences. Firms can steer adaptation in both directions. When workers bear adaptation costs privately, their individually chosen level of adaptation may be inefficiently low from the firm's perspective, giving firms incentives to encourage adaptation—for example, by covering the additional fuel costs associated with air conditioning use. At the same time, because firms also face the risk that workers may overuse adaptation due to moral hazard, they may restrict other adaptation margins, such as excessive rest or work absences taken under the pretext of heat exposure. The extent to which firms steer adaptation and the specific margins they target, therefore, depend on the trade-off between the benefits of adaptation and the risk of moral hazard.[5]

To formalize these ideas, we develop a structural model of firm-steered adaptation that captures the main empirical patterns and the trade-off described above. We calibrate the model to moments from our empirical estimates and use it to simulate counterfactuals under alternative firm policies and varying degrees of moral hazard. The model shows that, absent firm steering, employee drivers would make 14.3% more heat-induced mistakes than owner-operators, indicating that firm's sharing of adaptation consequences, without effective steering, can worsen performance through moral hazard. Comparing

[5]We define moral hazard as distortions in adaptation behavior that arise when workers' adaptation choices are (i) not fully contractible, because perceived heat exposure is driver's private information, and (ii) the costs or consequences of those choices are partially shared with the firm.

this counterfactual to the observed outcome further shows that firm steering offsets 62.5% of the heat-induced mistakes that would otherwise arise.[6]

Our findings have several policy implications. First, workplace heat policy should account for differences across labor contracts rather than rely on one-size-fits-all protections, since workers who bear operating costs directly face stronger barriers to adaptation and may require more targeted support. Second, employer involvement can improve adaptation, but the relevant policy objective is not simple cost sharing alone; rather, policies should encourage incentive-compatible firm responses, such as documented heat-response plans, monitoring, dispatch adjustments, and verifiable cooling and rest protocols. Third, policy evaluation could also account for firms' ability to partially smooth heat shocks by reallocating labor, implying that worker-level safety and productivity losses may remain substantial even when firm-level output appears less affected.

Related literature and contributions. This paper contributes to several strands of literature. First, it closely relates to the growing body of research on the impacts of extreme temperatures and individual adaptation. Existing studies have documented significant adverse effects of heat exposure and examined adaptation across various contexts, including agricultural production (Burke and Emerick, 2016; Cui, 2020; Cui and Xie, 2022; Patel, 2024), health outcomes (Deschênes and Greenstone, 2011; Barreca et al., 2016; Heutel, Miller and Molitor, 2021), human capital formation and performance (Park et al., 2020; Garg, Jagnani and Taraz, 2020; Sexton, Wang and Mullins, 2022), and firm operations (Pankratz and Schiller, 2024; Balboni, Boehm and Waseem, 2024; Grover and Kahn, 2024). By providing the first empirical evidence on how extreme temperatures influence driving behaviors, we contribute novel insights on adaptation in the transportation sector – a critical yet under-explored setting.

Unlike prior studies, we examine a context where heat-induced performance declines create substantial negative externalities, and adaptation investments can yield broader public benefits. Our findings show that private adaptation investments often fall short of socially optimal levels, underscoring the importance of cost-sharing schemes and financial incentives in shaping adaptation outcomes. Additionally, we contribute to the literature on differential access to and investment in adaptation (Baylis and Boomhower, 2021; Davis et al., 2021; Park, Pankratz and Behrer, 2021) by offering potential explanations.

[6] All quantities refer to the estimated effect of one additional hour above 33°C on the number of dangerous driving behaviors. The observed effects are 0.7 for owner-operators and 0.3 for employee drivers, while the no-steering counterfactual for employee drivers is 0.8. Hence, 14.3% is given by $(0.8 - 0.7)/0.7$, and 62.5% by $(0.8 - 0.3)/0.8$.

Methodologically, we advance this literature by leveraging granular data at the individual route (or trajectory) level, rather than relying on aggregated analyses by jurisdiction, administrative region, or road segment. Using more granular data in a fixed-effects panel model not only reduces vulnerability to different-frequency issues and data aggregation bias, as highlighted by Ghanem and Smith (2021) and Cui et al. (2024), but also enables us to exploit richer variations by constructing flexible exposure measurements. Similar GPS and route data have been increasingly used in both environmental (Xia et al., 2023), trade (Barnwal et al., 2024), and urban transportation economics literature (Alder, Song and Zhu, 2023; Chen et al., 2025). The innovation of our data is that it includes not only real-time GPS pings but also direct observations of driver behavior captured by cameras and sensors and the personnel information. This enables us to explore the mechanisms underlying behavioral responses and institutional arrangements.

This paper also contributes to the empirical literature on contracting, moral hazard, and organizational governance. In the U.S. trucking industry, Hubbard (2003); Baker and Hubbard (2003, 2004) show that information and monitoring technologies shape productivity, asset ownership, job design, and governance by changing what can be observed and contracted upon. These papers make clear that the distinction between owner-operators and firm-employed drivers is not unique to China, but reflects a broader make-versus-buy problem under imperfect information. We show that this organizational margin also matters for climate adaptation: under extreme heat, contract form shapes not only performance outcomes but also the specific margins through which workers adapt. More broadly, the paper relates to Laffont and Matoussi (1995); Burchardi et al. (2019), which show that shared contractual arrangements can distort behavior through moral hazard. We extend this literature to worker adaptation under climate risk, where adaptation choices are imperfectly contractible, perceived heat stress is partly private information, and firm involvement creates a trade-off between improved risk sharing and moral hazard. The paper also connects to recent evidence that monitoring technologies shape firm-worker relationships and contract implementation (Kelley, Lane and Schönholzer, 2024).

Outline. This paper is organized as follows. Section 2 introduces the background related to the transportation industry in China, driving monitoring systems, and drivers' adaptation behaviors. Section 3 discusses data used in this study. Section 4 discusses the construction of heat exposure measurements and empirical designs. Section 5 displays estimation results and heterogeneity. Section 6 discusses the implication of findings based on a simple model. Section 7 concludes.

2 Background

2.1 Transportation Industry in China

In China, the heavy-duty cargo transportation sector moves 40.3 billion tons of goods each year, accounting for 73% of the total goods handled by the logistics industry (Ministry of Transport of China, 2024). The industry operates 11.67 million trucks and employs 3.3 million truck drivers, representing 54% of the workforce in the cargo transportation sector.[7] As a comparison, US cargo transportation sector moves 20.2 billion tons in 2023 and 3.6 million truck drivers.[8]

Truck drivers must comply with regulations designed to improve road safety and traffic flow. For instance, drivers of commercial freight and hazardous goods vehicles are prohibited from exceeding load limits and cannot drive for more than four consecutive hours.[9] Additionally, truck operations are restricted by time and location in certain cities, with each municipality enforcing its own rules.[10]

In 2023, the median income for truck drivers in China is approximately $18,000, which is close to the national average wage of $17,242.57. In comparison, the median income for truck drivers in the US is estimated to be $70,000 (ATA, 2021).

2.2 Accidental Risks of Heavy-duty Trucks

Truck transportation has the highest fatality rates among all transportation modes. In 2022, there were 256,409 road accidents in China, resulting in 42,021 deaths and 149,650 injuries.[11] Trucks account for 8% of total automobiles but 30% of traffic fatalities (China Traffic Administration Bureau, 2013). Based on the Large Truck and Bus Crash Facts compiled by US Department of Transportation (DOT), during 2012 - 2021, during 2012–2021, the involvement rate per 100,000 registered large trucks was 37.664, and per 100 million vehicle

[7] Source: China Statistical Yearbook 2023.

[8] Source: Freight Facts and Figures by Department of Transportation and Drivers Resource Center.

[9] According to the "Road Transport Vehicle Technical Management Regulations" and the "Road Transport Personnel Management Regulations," strict limits are imposed on continuous driving time to prevent fatigue. Specifically,

[10] In Guangzhou, for example, trucks are banned from certain city center roads during morning and evening rush hours. The Guangzhou Tunnel and the Zhonghuan East and West Roads in Guangzhou University Town are closed to truck traffic all day. The Liuhua area prohibits truck traffic from 7 am to 10 pm daily, and specific sections of Zhongshan Road and the Luoxi Bridge are also restricted to trucks at designated times.

[11] Source: China Statistical Yearbook 2023.

miles traveled (VMT) was 1.549. Over this period, 45,400 trucks were involved in fatal crashes, resulting in 46,283 fatalities. Among these, 13,037 were truck occupants, while 33,246 were occupants of other vehicles or non-occupants.

Trucks are dangerous because they are heavy. Being hit by a vehicle that is 1,000 pounds heavier generates a 40–50% increase in fatality risk (Anderson and Auffhammer, 2014). As a result, the risk of truck accidents also poses significant externalities to other vehicles on the road. For these reasons, trucks are often referred to as "road killers."

Another reason why trucks are dangerous in China is that the overtime and night-time hours for heavy-duty truck drivers in China are excessively long. During our sample period, the average driving hours (hands on the wheel) are about 8 hours. Even when not driving, the truck drivers have excessively long on-duty hours of more than 19 hours. Therefore, drivers tend to eat and sleep in the truck.

Based on the Large Truck and Bus Crash Facts, among driver-related factors, speeding was the most common, followed by distraction (e.g., cell phone use, being lost in thought, eating) and careless driving as the second and third most frequent driver-related factors.

2.3 Relationship Between Truck Drivers and Company

Most local governments in China do not allow individuals to operate heavy-duty trucks independently. As a result, freight transportation is typically organized through licensed trucking companies or truck fleets, and truck drivers generally work under one of two arrangements: as employee drivers or as affiliated contractors.

Employee drivers have formal labor contracts with trucking companies. They operate company-owned trucks, receive assignments from dispatchers or fleet managers, and are generally required to follow firm-assigned routes and schedules. The company pays wages and commissions, provides social insurance, and covers major operating expenses, including fuel, maintenance, depreciation, and transportation insurance.[12] Affiliated contractors, by contrast, typically operate under the company's brand while owning their own trucks. They pay a management fee to the company, retain the revenue from their own operations, and have greater discretion over task acceptance, route choice, and work schedules. They also bear their own operating expenses, including fuel, maintenance, insurance, and vehicle depreciation.

[12]Chinese transportation regulations require trucks operating on public roads to carry compulsory motor vehicle third-party liability insurance.

These two arrangements imply different pay-setting and risk-bearing structures. For employee drivers, earnings are determined mainly by wages and commissions set by the firm, so realized income is relatively stable and only indirectly linked to trip-level costs. For affiliated contractors, net earnings depend on both revenue and realized operating expenses, making pay more sensitive to route choice, work intensity, and market conditions. In our interviews, fuel costs alone account for more than 40% of total operating expenses for affiliated drivers. More broadly, truck driving in China is not a high-wage occupation on average: in 2023, the median annual income of truck drivers was about $18,000, close to the national average wage of $17,242.57, while the corresponding figure in the United States was around $70,000.

The two arrangements also differ in accident-related risk and insurance coverage. When employee drivers are involved in accidents, compensation and claims are typically handled through the firm and its insurance arrangements, and company support may include wage protection, legal assistance, and replacement vehicles. Affiliated contractors, by contrast, must purchase and maintain insurance on their own and remain more directly exposed to repair costs, liability, and income interruptions following accidents. Compulsory insurance provides only limited third-party coverage, so broader commercial insurance remains important in practice, especially in heavy-duty trucking where potential losses can be large.

2.4 Adaptation Behaviors and Costs

Truck drivers could adapt to the temperature shock in several ways, but all these adaptation behaviors come with monetary costs or opportunity costs.

Air Conditioning. The most direct and effective adaptation behavior is turning on the vehicle air conditioning (AC) system. However, using air conditioning could substantially increase fuel consumption and expenses. Existing studies and anecdotal evidence have shown that operating the AC cooling system puts an additional load on the engine, as it requires extra power to run the compressor, leading to increased fuel consumption.[13] According to the U.S. Environmental Protection Agency (EPA)'s and Department of Energy (DOE)'s guidance, AC usage can reduce a vehicle's fuel economy by more than 25%. A bolder estimation by the U.S. National Renewable Energy Laboratory (NREL) in the early 2000s indicates that AC systems can reduce the fuel economy of high fuel-economy vehicles

[13] Anecdotal evidence from automotive user Apps can be found *here* and *here*.

by about 50% (Farrington and Rugh, 2000; Rugh, Hovland and Andersen, 2004). More rigorous estimations from automobile and thermal engineering studies convey numbers of similar magnitude (Huff, West and Thomas, 2013; Lee et al., 2013; Wu et al., 2022). Therefore, using a conservative estimation, the fuel consumption of a truck would increase by about 25% after the air conditioning is turned on.

At the same time, fuel (diesel) expenses are one of the major costs for operational trucks, which could account for about 50% of the total operational cost.[14] Therefore, to save fuel and reduce operating costs, truck drivers who are responsible for covering their own fuel expenses (e.g., contractors in our context) may opt not to use the AC system, particularly when the cargo does not require temperature control. Although we do not directly monitor vehicles' AC status, the hypothesis that truck drivers do not always turn on the AC can be indirectly supported by snapshots from our raw DMS system data. As Appendix Figure D4 shows, the camera originally installed to capture drivers' facial information also recorded instances where the cabin window was open. This suggests that, at those moments, the drivers were likely not using the AC system.

Rest and Working Schedule. Another direct adaptation behavior is to increase rest or adjust work schedules. Drivers may take more frequent or longer rests, for example in shaded or naturally cooler areas or at designated rest stops along highways, which allows them to recover from heat exposure. The main cost of this behavior is the opportunity cost of time spent resting, which may reduce the total number of shipments completed. In our data, we measure resting behavior by identifying consecutive time intervals during which trucks remain at the same location with zero speed throughout the period.[15]

Adaptation may also occur through changes in the timing of work. On hotter days, drivers may choose not to work, start work later than usual, or shift driving activity away from the hottest hours of the day. These responses can mitigate heat exposure but may also reduce daily output. We measure this margin using indicators for whether the driver works on a given day, the daily work start time conditional on working, and the within-day timing of driving activity. These measures allow us to separately capture adaptation through rest and adaptation through broader changes in working schedules.

[14] According to China 2021 Road Freight Industry Key Enterprises Operational Report by China Federation of Logistics and Purchasing, toll fees, fuel costs, driver wages, and vehicle depreciation are the four main expenses, accounting for 32.1%, 30.1%, 19.7%, and 13.3%, respectively. In terms of operational cost (variable cost), fuel expenses account for about 48.4%.

[15] GPS records location and motion data even if the vehicle engine is not started. Therefore, we have 24-hour complete records for every vehicle every day.

Route choice and tasks Qualitative data from interviews with both contract and employee drivers reveal significant discretion in their operational decision-making, particularly concerning route selection. Drivers of both employment types reported that their route planning is primarily driven by the optimization of time and fuel costs, rather than environmental factors. While employee drivers are constrained by company-imposed limits on toll expenditures, the fundamental economic calculus of their routing decisions remains the same. Notably, ambient temperature was not reported as a consideration in their route planning; no drivers indicated they would avoid certain routes due to heat. This operational autonomy extends, albeit unevenly, to task selection. Employees typically operate between a set of predefined destinations, whereas contractors possess greater latitude, with their destinations being contingent upon the specific tasks they accept from freight platforms. Even with this freedom, contractors affirmed that temperature does not influence their choice of assignments, reinforcing the finding that immediate economic and logistical efficiencies are the dominant factors in their daily operational choices.

3 Data

This paper combines detailed GPS and truck monitor sensor data with high-resolution weather conditions and air pollution monitor data. We discuss each data source as follows.

3.1 Real-Time Truck Monitoring System

A real-time truck monitoring system is a driving assistance system aimed at detecting dangerous driving behaviors and preventing truck fleet accident risks. For commercial vehicles, installing such monitoring systems and connecting to the government platform is required by the Guangdong provincial government, regardless of whether the driver is a contractor or a non-contractor. We work with a smart driving company that offers monitoring services to truck fleets. These services are aimed at cargo companies in Guangdong, China. The company installs sensors and cameras and uses facial recognition technology to identify risky driving behaviors. It also sends immediate alerts to address potential dangers.

The systems for detecting risky driving can be divided into three groups: Driver Monitoring Systems (DMS), Advanced Driver Assistance Systems (ADAS), and Blind Spot Detection (BSD). DMS is camera-based system that watches the driver's face and eyes. It detects fatigue or distraction and issues warnings to prevent accidents caused

by inattention (see examples in Figure D2); ADAS is a sensor-based system monitors the vehicle's surroundings. It alerts drivers about lane departures, potential collisions, and other risks; BSD use sensors to check blind spots around the vehicle. It warns drivers about nearby objects or vehicles, helping to prevent accidents due to limited visibility. Figure D3 shows how BSD works, using the right blind spot as an example.

The system is designed to provide immediate, real-time alerts to the driver when it detects signs of fatigue, distraction, or other unsafe behaviors. For instance, if it notices the driver's eyes closing frequently or their head nodding due to tiredness, it will trigger an alarm instantly. These alarms usually come as auditory signals, like a beeping sound, to ensure the driver is notified quickly and effectively. Drivers are aware of the system and have received the necessary training.[16]

This company is one of the suppliers for the government. In February 2021, the Guangdong government launched an integrated intelligent monitoring and alarm platform. This platform aims to detect and prevent road traffic safety risks in a systematic way.[17] The government sets the standards, while partner companies handle the production, installation, and continuous maintenance of the devices.

3.2 Real-time GPS and Warning Data

Our dataset includes around 10,000 heavy-duty trucks and truck drivers, and approximately 130 freight companies, covering the sample period from March 2023 to June 2024. Every truck in our dataset is installed with real-time GPS sensors that record geocoordinates (longitude and latitude), direction (in angles from 0 to 360), instantaneous speed (km/h), and engine status (activated or inactivated). Our data records GPS sensor readings every 20 seconds when the truck is moving and every 2 minutes when the truck remains not moving. Each reading in the raw data corresponds to a geocoded point with the variables mentioned above. Similar real-time GPS reading data have been used by previous studies on congestion and traffic flows (Alder, Song and Zhu, 2023; Chen et al., 2025). In addition to regular interval observations, our data also include additional GPS readings

[16] If a driver is often flagged by the monitoring system, the consequences can be serious, especially if it leads to accidents. These consequences can include warnings and feedback aimed at improving driving habits. In more severe cases, drivers may face fines or even dismissal if their unsafe behavior is repeated. These actions are taken to ensure drivers follow safety regulations.

[17] Guangdong Province has successfully tracked and monitored 760,000 business-purpose vehicles. The government uses this data to send daily alerts about high-risk vehicles and their registered companies. Since these reforms started, road traffic accidents have decreased by 71%, and fatalities have dropped by 69% for monitored vehicles compared to 2019. Sources: Ministry of Transport of PRC (in Chinese).

whenever a sensor warning is triggered. For these incidental readings, we observe the exact type of warning and the corresponding sensor that triggered it.

A unique feature of our data is that we observe warnings from sensors installed on the truck to measure dangerous driving behaviors directly. The data comes from the full recording of the Driver Monitoring System (DMS), Advanced Driver Assistance Systems (ADAS), and Blind Spot Detection (BSD). These systems are integrated to form the complete truck driving monitoring system. The DMS employs an in-cabin camera to monitor the driver's face and eyes, detecting signs of fatigue or distraction through artificial intelligence techniques based on facial recognition and tracking algorithms. For example, if a driver is detected with a wide-open mouth, the algorithm identifies it as yawning, which is then classified as fatigued driving. As long as a pre-defined behavior is detected, the camera will upload the snapshot photos to the system background. Figure D2 shows three examples of snapshots. The ADAS sensors are mainly installed outside the vehicle and capture incidents such as blind spot detection, lane departure, and following too closely, etc.

Table 1 reports descriptive statistics for daily aggregated outcomes derived from real-time GPS and warning data. On average, a driver triggers 13 warnings for every 100 km of driving. Blind spot warnings represent the largest share, accounting for approximately 40% of all warnings. Among warnings captured by inside-cabin sensors, distraction is the most frequently recorded category.

Figure D5 displays the number of warning records per hour over the course of an example day. Two patterns emerge from this figure. First, the number of warnings from outside-cabin sensors (ADAS and BSD) exceeds those from inside-cabin sensors (DMS). The top three warnings from outside-cabin sensors are right blind spot, collision, and lane departure warnings.[18] Second, the number of warnings is higher during the middle of the day, when the temperature is highest, which suggests a correlation between temperature and dangerous driving behavior.

3.3 Weather and Pollution Data

Weather. We collect weather data from the ERA5-Land reanalysis dataset provided by the European Centre for Medium-Range Weather Forecasts (ECMWF). Reanalysis data are generated by integrating atmospheric models with local station observations. ERA5-Land

[18]China is a left-hand drive country, meaning the driver and steering wheel are positioned on the left side of the vehicle. Therefore, the right blind spot is the major blind spot.

offers global hourly surface weather data on a $0.1^\circ \times 0.1^\circ$ grid (approximately 9×9 km) dating back to 1950. For this study, we identify grids within Guangdong province and extract a range of weather variables –including air temperature, dew point temperature, precipitation, wind speed, and wind direction – for the period from March 2023 to June 2024. Compared to ground monitoring station data, ERA5-Land provides higher spatial granularity, allowing us to better capture spatial variations in weather conditions. Figure 1(a) plots the grid locations along with the corresponding average daily temperatures. Over the sample period, the average temperature ranges from 16° to 28° across grid locations.

In addition to these key weather conditions, we assemble from the ERA5 dataset additional meteorological variables and surface characteristics from the ERA5 dataset, such as UV radiation, total cloud cover, vegetation cover, and leaf area index, which are primarily used as controls. Although the ERA5 dataset offers a broader range of variables, it has a coarser spatial resolution of $0.25^\circ \times 0.25^\circ$. To harmonize the spatial resolutions of the two datasets, we apply linear interpolation to refine the ERA5 data to match the resolution of ERA5-Land.

Air Pollution. China began real-time automatic air pollution monitoring in 2013. We collect hourly air pollution data, including the Air Quality Index (AQI) and pollutant concentrations, from all 154 monitoring stations in Guangdong province for the period between March 2023 and June 2024. To integrate these station-level records with other datasets, we interpolate the pollution measurements onto a $0.1^\circ \times 0.1^\circ$ grid using the nearest neighbor method.

3.4 Auxiliary Data

Personnel Information. To acquire information about the relationship between the truck fleet, either as an employer-employee relationship or a contractor arrangement, we conduct a phone call interview of all truck companies that install the truck sensor provided by our collaborated company.[19] If the company has contractor drivers, then the company would be categorized as a contractor arrangement. If all drivers are employed by the company, then the company would be categorized as an employer-employee arrangement (non-contractor). We successfully gathered data on 104 trucking companies, whose trucks account for approximately 37.3% of all trucks in our sample.

[19] In our context, depending on the type of fleet business, the relationship between the fleet and the driver is likely to be consistent.

Truck Fleets Information. We collect information about the type of business and the type of cargo carried by the truck fleets, combining phone call interviews with manual searches through a Chinese enterprise information platform.[20] The type of business is categorized based on the industrial classification for national economic activities. Specifically, we use this classification to distinguish between passenger transportation and goods transportation. In terms of cargo type, general merchandise, seafood, steel, sand and soil, and electronics are classified as non-hazardous cargo, while liquefied petroleum gas, gas cylinders, chemicals, and other flammable and explosive hazardous materials are classified as hazardous cargo.

Geographic Characteristics. We collect elevation and slope data from the ASTER Global Digital Elevation Model Version 3, which provides a global elevation model at a spatial resolution of approximately 30 meters. Additionally, we obtain data on water features, such as rivers and lakes, from OpenStreetMap. To measure road conditions, we overlay these geographic layers onto daily routes to calculate the average elevation, slope, and proportion of water areas along each route.

GIS data. We compile Geographic Information System (GIS) data on administrative jurisdiction boundaries and road networks in Guangdong Province based on geocoded maps from National Platform for Common GeoSpatial Information Services.

4 Empirical Design

4.1 Constructing Route-Based Temperature Exposure

One empirical challenge of this paper is to measure drivers' exposure to temperature shocks while they are moving across large spatial areas. In the canonical context of the temperature literature, the object of interest typically remains within a fixed location or jurisdiction area throughout the study period.[21] In these scenarios, researchers match the object's fixed location or jurisdiction with weather records within that region. Temperature exposure is then measured by averaging data across the corresponding spatial area.

[20] Source: https://www.tianyancha.com.

[21] Most studies assume the object moves but primarily within specific administrative boundaries (e.g., counties or cities). In such cases, data is aggregated at the level of these jurisdictions, and information on spatial movements within the boundaries is omitted.

Our context differs from previous studies due to the high granularity of our data, both spatially and temporally, as we observe drivers' locations every twenty seconds. Consequently, within the typical time intervals for which weather records are available (e.g., one hour or three hours), a driver's route often spans multiple locations. One potential solution is to aggregate the data to a spatial unit with fixed geographic boundaries, such as a city or county, and measure the temperature exposure by averaging over the entire region. However, estimating temperature effects using such aggregated temperature exposure over large spatial areas may cause bias due to non-classical measurement error (Carson and Yu, 2024) or the presence of unit-specific response heterogeneity (Ghanem and Smith, 2021). In our specific context, this approach could overlook important spatial variations in temperature and fail to capture the dynamic cumulative effects of heat exposure on driving behaviors.[22]

We overcome the challenge by extending the standard measurement and constructing route-specific temperature exposures. Figure D1 illustrates our approach. Specifically, for a driver i, we sequentially connect all GPS locations (blue points) and warning-triggered locations (red points) based on their timestamps. This generates a route within each time interval of the ERA5-Land data (i.e., one hour in our setting). Next, we overlay the route with the ERA5-Land grid and identify the set of overlapped pixels during hour h on day t, denoted as $\mathcal{P}_{ht}$.[23] For each pixel $p \in \mathcal{P}_{ht}$, we calculate the duration (or driving distance) associated with the overlaid route segment, denoted as d_{ipht}. Each pixel p has a specific temperature reading T_{pht}. We assign T_{pht} into a set of temperature bins $\mathcal{B} = \{[\leq 6°\text{C}], [9-12°\text{C}], ..., [30-33°\text{C}], [> 33°\text{C}]\}$, and define the duration of driver i's exposure to temperature in bin $k \in \mathcal{B}$ for hour h on day t as follows:

$$d_{iht}(k) = \sum_{p \in \mathcal{P}_{ht}} d_{ipht} \cdot \mathbb{1}[T_{pht} \in k].$$

In the main specification, for computational efficiency, we aggregated the data for each driver by date, making the unit of observation a driver-day. We show in the Appendix that our main findings are robust when the data is instead aggregated to the driver-by-hour level.

With the daily sample, we construct two measures of temperature exposure. First, to characterize the distribution of temperature exposure within a day, we calculate the

[22] For example, if a warning is triggered when a driver passes through city A, this approach might incorrectly attribute the warning to city A's temperature, even if the associated dangerous driving behavior is caused by cumulative heat exposure along the route outside city A.

[23] In this example, $|\mathcal{P}_{ht}| = 4$.

number of hours with temperature exposure falling into each bin:

$$D_{it} = \left\{ d_{it}([\leq 6^{\circ}\text{C}]), d_{it}([6-9^{\circ}\text{C}]), ..., d_{it}([30-33^{\circ}\text{C}]), d_{it}([>30^{\circ}\text{C}]) \right\},$$

where

$$d_{it}(\cdot) = \sum_{h} d_{iht}(\cdot).$$

Figure 1(b) plots the average number of hours per day that drivers are exposed to temperatures within each bin. Guangdong is located in a hot climate region and drivers on average experience temperature exposure above 24°C for more than half of a day. The advantages of this measure is that it fully leverages the high granularity of our data, capturing rich variations in temperature exposure across different times and locations. Compared to prior panel-data studies that primarily use regional temperature anomalies, our approach accounts for the temperature variation stemming from the combination of various locations formed by truck routes spanning large spatial areas. This richness in variation, as we will explain in the next section, is important for identifying the nonlinear effects of temperature exposure.

In addition to the binned temperature measures, we also calculate the duration-weighted average temperature exposure in a day as:

$$T_{it} = \sum_{h} \frac{d_{ipht}}{\sum_{p \in \mathcal{P}_{ht}} d_{ipht}} \cdot T_{pht}.$$

Using the same approach, we compute drivers' weighted average exposure to various meteorological and road conditions, such as precipitation, wind speed, slope, elevation, etc.

4.2 Econometric Model

Temperature effects on driving and adaptation behaviors. For sensor i on date t, we estimate the following model to examine the non-linear effects of temperature exposure

on driving behavior:

$$Y_{it} = \underbrace{\sum_{k \in \mathcal{B}} \rho^k d_{it}(k)}_{\text{temperature distribution}} + \gamma' \mathbf{X}_{it} + \alpha_i + \delta_t + \varepsilon_{it}, \tag{1}$$

where the outcome of interest Y_{it} is modeled as a function of the duration of temperature exposure $d_{it}(k)$, which is defined as the number of hours in a day with exposed temperature falling into specific bins $k \in \mathcal{B} = \{[\leq 6°\text{C}], [6-9°\text{C}], ..., [30-33°\text{C}], [> 33°\text{C}]\}$. We omit the duration for temperature bin $[18-21°\text{C}]$ and regard it as the reference category. The parameters of interest ρ^k capture the effect of an additional hour of exposure to temperatures in bin k,relative to exposure to temperatures in the reference category, i.e., 18-21°C.[24]

We control for a comprehensive set of route-specific variables, $\mathbf{X}_{it}$, including topographical characteristics like average elevation and slope; pollution exposure measured by average AQI; and average exposure to other meteorological conditions, such as precipitation, wind speed and direction, among others. The average pollution and weather controls are constructed in the same way as the average temperature exposure. To allow for non-linearity, we include quadratic terms for average precipitation and wind speed in the model.

We include sensor-device fixed effects α_i and date fixed effects δ_t. During our sample period, changes in drivers and trucks are rare; therefore, α_i effectively also controls for driver-by-truck fixed effects. In the Appendix, we demonstrate that the results are robust to alternative combinations of time fixed effects. In the context of our study, delivery destinations and routes are determined by the shipping company, making it unlikely for drivers to select routes based on the spatial distribution of heat. Therefore, the temperature exposure measure can be considered exogenous to other factors influencing driving behaviors, particularly after controlling for time and truck fixed effects. Standard errors are clustered at the device level.

To account for potential spatial differentiation between routes – such as differences between urban and rural areas or plains and mountainous regions – we conduct a robustness

[24]Our specification exploits the within-variation in distribution of temperature exposure within a day instead of average temperature exposure. Intuitively, consider a simple example of two drivers A and B in a day, both of them drive for 10 hours and the average temperature exposure of 24°C. Driver A drives in 24°C conditions for 10 hours. Driver B, however, experiences more fluctuating heat exposure, driving in 18°C for five hours and 30°C for another five hours. Using the duration of exposure to temperatures in each category, we are comparing whether driver B makes more mistakes due to longer exposure to temperatures 30°C.

check and show that the coefficient estimates remain largely unchanged when including route-specific spatial dummies indicating whether the route crosses specific regions.

5 Results

5.1 Effects of Heat Exposure on Dangerous Driving Behaviors

We first present baseline regression results estimated using Equation 1. Figure 2 plots the temperature response function for the intensity of alarms, measured by the number of alarms per 100 km of driving. Blue dots are point estimates and gray caps are associated 95% confidence intervals. Estimates are relative to temperature between 18-21°C, i.e., the omitted reference group, and are shown for each temperature bin in degrees Centigrade.

We find that the intensity of dangerous driving behaviors increases during hot temperatures relative to mild ones. For temperatures above 27°C, the number of alarms per 100 km rises notably, with the effect becoming particularly pronounced at temperatures above 33°C. The effects of extremely high temperature (above 33°C) are positive and statistically significant. The point estimate suggests that an extra hour with temperature exposure higher than 33°C increases the number of alarms by 0.4 per 100 km of driving, compared to an hour of exposure between 18-21°C. Given that the average daily alarm intensity for a sample driver is 13.2 per 100 km of driving, this corresponds to a 3% increase in the incidence of dangerous driving behaviors for the average driver.

The implied costs from heat-induced dangerous driving behaviors are economically significant. To quantify the monetized losses, we calibrate the elasticity of crashes to dangerous driving behaviors using data from the US DOT's Large Truck and Bus Crash Facts. Our findings indicate that a 3% increase in dangerous driving behaviors corresponds to a 2.4% rise in accidents for a sample truck driver. At the aggregate level, there were 43,444 truck-related accidents in 2023, resulting in $11.67 billion in losses. Based on our estimate, if all truck drivers were to jointly experience an extra hour with temperatures above 33°C instead of 18–21°C, the total number of accidents would increase by 1,042, with economic losses rising by $280 million. Detailed calculations of the monetized costs are provided in Section 5.7.

5.2 Mechanisms and Heterogeneity

5.2.1 Extensive vs Intensive Margins

The heat-induced alarms may stem from two distinct channels: the extensive margin, where more drivers trigger alarms during hot temperatures, and the intensive margin, where individual drivers trigger a greater number of alarms. Figure D7 presents the estimated effects of temperature on the two margins separately. The left panel captures the extensive margin by estimating the effect of temperature on the likelihood of a driver triggering any alarms in a day. The results indicate that temperature has minimal impact on the extensive margin - the probability of a driver triggering at least one alarm remains statistically indistinguishable from zero across all temperature ranges.

In the right panel of Figure D7, we estimate the effect of temperature on alarm intensity, restricting the sample to observations with at least one alarm in a day. The results reveal that temperature strongly affects the intensive margin among drivers who trigger alarms. For these drivers, the number of alarms per 100 km increases dramatically at higher temperatures. This pattern suggests that the surge in dangerous driving behavior during hot weather is primarily from increased safety violations among drivers who already exhibit compromised driving habits, rather than from a broader deterioration in driving safety across the population. Specifically, while the proportion of drivers receiving safety alerts remains constant, the frequency and severity of their dangerous driving incidents escalate significantly under extreme heat conditions.

5.2.2 Inside-Cabin vs Outside-Cabin Behaviors

To understand the driving behaviors that trigger these safety alarms, we disaggregate our analysis by alarm type and estimate the temperature effects separately. Alarms are first classified into two broad groups: those related to outside conditions, captured by the vehicle's external sensors, and those related to inside conditions, monitored by the interior camera. Next, we further decompose these alarms into specific categories. This classification allows us to examine how extreme temperatures influence both external driving challenges and internal driver behaviors.

For ease of interpretation and comparison, Table 2 reports the estimated coefficients for each alarm category, focusing only on the $>33^{\circ}$C temperature bin.[25] These estimates

[25]The full set of coefficient estimates for all temperature categories is presented in Figure D6.

capture the relative change in the number of alarms per 100 km of driving associated with one additional hour of temperature exposure above 33°C, compared to exposure within the 18-21°C range. Results are presented separately for alarms related to outside conditions (columns 1–5) and inside conditions (columns 6–8).

Among alarms associated with drivers' responses to outside conditions, blind spot alarms exhibit the largest increase under extreme heat (>33°C). Extreme heat also raises the likelihood of aggressive driving, as evidenced by increases in alarms due to following too closely, collision risks, and lane departures. These findings suggest that extreme heat significantly impairs drivers' spatial awareness and their ability to maintain safe distances from other vehicles. In contrast, speeding alarms, which occur much less frequently, exhibit a slight decrease, possibly indicating that drivers moderate their speed during extreme heat conditions.

For inside conditions, exposure to extreme heat significantly increases alarms related to impairments in drivers' cognitive and physical performance. During hot temperatures, drivers are more likely to become distracted, such as by checking their cellphones, making phone calls, or smoking, which reflects a diminished ability to maintain focus. We also observe a significant increase in alarms associated with fatigued driving, suggesting that extreme heat intensifies physical exhaustion, which can impair reaction times and decision-making. Additionally, alarms for hands-off steering wheel, though less frequent, also rise, signaling a loss of control or attentiveness in critical situations. These results highlight how extreme heat impairs drivers' performance internally, by directly affecting their concentration, alertness, and physical engagement with the vehicle.

To compare the total effects on behaviors related to outside versus inside conditions, Figure D8 shows the estimated effects of temperature on these two groups of alarms. Alarms related to outside conditions increase significantly at temperatures above 27°C. In contrast, alarms related to inside conditions remain stable across most temperatures but rise sharply when temperatures exceed 33°C. Notably, over 80% of the alarms triggered during extreme heat (>33°C) are related to outside conditions.

5.2.3 Safety Protocols and Perceived Accident Costs

Extreme heat may have differential impacts on driving behaviors due to variations in safety protocols, regulatory oversight, and risk perceptions across transport categories. For instance, passenger transportation and hazardous cargo operations often involve stricter regulations, higher stakes, and more severe accident consequences as perceived by drivers.

These factors likely incentivize more cautious driving compared to non-passenger or non-hazardous transport. To explore these heterogeneous responses, we classify vehicles based on their company's business scope and estimate temperature effects separately for each group.

Figure 3 examines the heterogeneity in alarm intensity by estimating the effects of temperature exposure across various transport categories. In Panel (a), vehicles are classified based on their company's business scope into passenger transportation (e.g., buses) and non-passenger transportation (e.g., freight or goods transport). The results indicate that while alarm intensity increases significantly for both groups at extreme temperatures, the effect is notably larger for non-passenger vehicles. In Panel (b), we categorize vehicles by cargo type, distinguishing those transporting hazardous goods (e.g., chemicals, flammable, or explosive materials) and those carrying non-hazardous cargo. Similar patterns emerge: vehicles carrying non-hazardous cargo exhibit markedly stronger responses to extreme temperatures compared to those transporting hazardous materials.

These heterogeneous effects suggest that the relationship between temperature and dangerous driving behavior varies systematically with the potential costs of accidents. Transport categories associated with higher accident costs – passenger transportation and hazardous materials – show more modest responses to temperature increases. This pattern is consistent with a risk-compensation framework, where drivers' behavior reflects the expected costs of accidents. When potential accident costs are high, as in passenger transport or hazardous cargo operations, drivers appear to maintain stricter safety protocols even under adverse conditions. Conversely, in operations where accident costs are relatively lower, drivers exhibit greater sensitivity to heat stress, likely due to reduced incentives to maintain rigorous safety practices under challenging conditions.

These findings highlight the interplay between economic incentives and environmental stressors in shaping workplace safety behavior. The results imply that existing regulatory frameworks and liability structures in high-stakes transport operations can effectively motivate sustained safety practices. However, additional interventions may be necessary in lower-stakes operations, where heat-related safety deterioration is more pronounced and regulatory oversight may be less stringent.

5.3 Effects of Heat Exposure on Productivity

Effects on Individual Work Load and Driving Speed. Extreme heat can impact drivers' productivity, influencing both the intensity and efficiency of their work. In the transporta-

tion sector, where time, distance, and speed are critical performance metrics, understanding how drivers adjust their work patterns under adverse environmental conditions has important implications for operational efficiency. To explore these adjustments, Figure 4 plots the estimated effects of temperature on various measures of driving activity, including driving distance, hours, and speed.

Panel (a) of Figure 4 shows the effects of temperature on daily driving distance and hours, both measured in logarithms. We find significant reductions in both metrics during extreme heat exposure. For driving distance, one additional hour of exposure to temperatures above 33°C leads to a sharp decrease of more than 4%. Given the mean driving distance of 150 km, this translates to an average reduction of 6 km per day. Similarly, driving hours decrease by approximately 2% with one additional hour of exposure above 33°C, equivalent to a 0.2-hour reduction in daily work time. These findings indicate that extreme heat substantially reduces drivers' overall work intensity, likely driven by heat-induced fatigue and associated safety concerns.

Panel (b) of Figure 4 shows the temperature effects on driving speed. Both mean and maximum speeds demonstrate significant declines during extreme heat. This reduction in speed, combined with the decreased work intensity, suggests that drivers adjust their behaviors comprehensively in response to heat stress. These adjustments align with compensatory strategies. Specifically, drivers respond to the physical and cognitive strain caused by extreme heat by reducing work intensity and driving speed, aiming to maintain safety under challenging environmental conditions.

Truck Company's Response to Mitigate Productivity Loss. How do transportation companies adjust their operations given the decline in individual drivers' productivity during extreme heat? To address this question, we aggregate the data to the company-by-day level, measuring total workload, the number of active drivers, and the average distribution of temperature exposure for tasks. Figure 5 reveals that while the total daily driving distance remains largely unchanged, transportation companies deploy more drivers on hotter days to maintain operational capacity. This suggests that companies respond to heat-induced productivity losses by redistributing tasks across a larger pool of drivers. This finding of managerial response to environmental shocks is consistent with that of in Adhvaryu, Kala and Nyshadham (2022).

5.4 Evidence on Adaptation Behaviors and Acclimation

Resting Behaviors. Drivers may adapt to extreme heat through both short-term adjustments and long-term acclimatization. Understanding these adaptive behaviors is crucial for evaluating how drivers navigate heat-related pressures and balance the trade-off between productivity and safety. Immediate responses, such as taking more frequent or longer breaks, represent a short-term strategy to manage heat stress. Over time, long-term acclimatization may lead to reduced sensitivity to heat exposure, particularly among more experienced drivers. In this section, we turn to exploring drivers' adaptation, in terms of both adjustments in resting behavior and differences in heat sensitivity.

Figure 6 presents the estimated effects of temperature on the frequency and average duration of rests. We classify rests into two categories based on their duration: short rests, lasting less than one hour, and long rests, lasting more than one hour. During extreme heat, short rests show a significant increase in frequency, but their average duration remains unchanged across temperature ranges, suggesting that drivers take more frequent quick breaks to manage heat stress. For long rests, we document a significant increase in both frequency and average duration during extreme heat. Specifically, with one additional hour of exposure of temperature above 33°C, the average duration of long rests increases by about 0.02 hours per 100 km of driving. To put this estimate in economic perspective, given the mean daily driving distance of approximately 150 km, if all 9,600 drivers in our sample were exposed to an additional hour of temperatures above 33°C, the cumulative time spent on rests would increase by 288 hours, equivalent to a loss of 36 standard workdays.[26] These results suggest individual driver's adaptation to heat stress can be costly and lead to notable productivity losses at the aggregate level.

Acclimation. Next, to examine long-term adaptation patterns, we analyze how temperature responses vary with drivers' historical heat exposure and baseline performance. First, we classify drivers into two groups based on whether their average temperature exposure during the sample period is above or below 24°C. Panel (a) of Figure 7 presents the estimation results. Drivers with greater exposure to hot temperatures are significantly less likely to trigger safety alarms during extreme heat compared to those with lower exposure. This suggests that regular exposure to hotter conditions may foster acclimatization, enabling these drivers to better deal with heat stress and maintain safe driving performance under extreme temperatures.

[26] The calculation assumes a standard workday consists of 8 hours of productive driving time.

In Panel (b) of Figure 7, drivers are classified, based on their average alarm intensity during mild temperatures (i.e., days with average temperature exposure $\leq 24^{\circ}$C), into high-performing group (those below the median) and low-performing group (those above the median). High-performing drivers show significantly fewer increases in alarm-triggering behaviors in response to hot temperatures, compared to low-performing drivers. This difference likely reflects their ability to maintain safer driving practices under extreme heat. High-performing drivers may possess greater driving skills, more experience, or better training, which enable them to adapt more effectively to challenging conditions caused by extreme heat.

5.5 The Role of Cost-Sharing Schemes

In our setting, the heavy-duty transportation industry features two distinct labor contract arrangements: independent contractors, who own their vehicles and bear all operational expenses, and company-employed drivers, whose operational costs are covered by their employers.[27] These arrangements imply different cost-sharing incentives and constraints, which in turn may shape drivers' adaptation responses to extreme heat. Relative to company-employed drivers, contractors face larger financial exposure and operational risk but enjoy greater flexibility in their work schedules. This institutional setting therefore allows us to examine how variation in cost-sharing arrangements and firm steering shapes both adaptation behavior and performance outcomes under extreme temperatures.

5.5.1 Differential Adaptation Responses

Air Conditioning and Ventilation. As we explain in Section 2, AC is one of the most effective ways to mitigate heat exposure for drivers. However, turning on the AC substantially increases fuel consumption for heavy-duty trucks. For contractors, as they bear all operating costs, they also bear the additional fuel cost from turning on the AC, while for employees, these additional costs are borne by the company. Therefore, we expect that differences in AC usage behavior may help explain the heterogeneous effects of heat exposure. However, our monitoring system does not record whether the air conditioning (AC) is turned on. To test the cooling strategy channel, we use the driver-side window opening status as a proxy for AC usage. The underlying assumption is that when the driver-side window is open, the AC is likely off. Thus, the probability of window opening is negatively and monotonically correlated with the likelihood that the AC is in use.

[27] Section 2.3 provides additional details on these two cost-sharing schemes.

To construct this variable, we train a computer vision algorithm and use it to classify 500,000 in-cabin camera images and detect whether the driver-side window is open or closed in each frame (see Appendix Figure D4 for example). We then match the window status data with contemporary weather conditions based on the time when each image was taken and the corresponding GPS location of the vehicle. We estimate the main specification and use the predictably probability of window opening as the outcome variable. Figure 8 shows that while both contractors and non-contractors are less likely to leave their windows open as temperatures exceed 24°C, contractors' window decisions are significantly less responsive to temperature increases. For non-contractors, the probability of driving with the window open declines sharply once temperatures exceed 21°C. Interestingly, contractors initially increase their window-opening behavior when temperatures rise from 18–21°C to 21–24°C, before eventually reducing it at even higher temperatures. This pattern suggests that contractors may initially rely on opening windows to cope with heat but switch strategies as temperatures become more extreme, likely due to diminishing cooling effectiveness or increasing discomfort from external air. These findings reinforce the idea that contractors, facing higher fuel costs, are more likely to forgo air conditioning as a cost-saving measure, making them more vulnerable to heat-induced driving risks.

We provide additional evidence that the heterogeneous responses between contractors and non-contractors are likely driven by differences in air conditioning usage.[28] Panel (a) of Figure D9 examines temperature effects by daily driving distance. We classify the sample into three groups based on drivers' daily driving distance: 0–100 km, 100–200 km, and >200 km. Drivers who travel longer distances are more likely to spend a greater proportion of their time on highways, where they must keep windows closed to reduce wind resistance, noise, and dust. This makes it more likely for them to turn on air conditioning for cooling. The results show that, for contractors, those driving longer distances exhibit reduced sensitivity to high temperatures compared to those driving shorter distances, as indicated by fewer alarms during extreme heat. For non-contractors, temperature effects across driving distances are mostly comparable, except when temperatures exceed 33°C. The pronounced reduction in alarms among contractors who driver longer distances likely reflects their higher reliance on air conditioning during highway driving.

Panel (b) of Figure D9 explores temperature effects under varying cloud cover conditions. Higher cloud cover reduces direct solar radiation, potentially lowering the perceived or "feels-like" temperature within the cabin and reducing the need for air conditioning. For

[28] Section 5.6 provides additional evidence that this heterogeneity is not attributable to differences in driver characteristics, exposure to diverse weather conditions, or transport categories.

contractors, alarm intensity during extreme heat is significantly lower on days with high cloud cover compared to days with low cloud cover. Notably, under high-cloud conditions, the effect of temperature on contractors is similar to that observed for non-contractors, implying that when in-cabin heat stress is less severe, the gap in adaptation behaviors between the two groups narrows. In contrast, non-contractors exhibit no meaningful differences in alarm intensity across cloud cover conditions.

Resting Behavior. Figure 9 examines differences in resting behavior between contractors and non-contractors under varying temperature conditions. Consistent with previous findings, both groups increase the frequency of short and long rests and the average duration of long rests during hot temperatures. However, these adjustments are significantly more pronounced among contractors. For instance, an additional hour of exposure to temperatures above 33°C increases the average duration of long rests among contractors by 0.08 hours (4.8 minutes), nearly four times the increase observed for non-contractors. The results reveal the more intensive adjustments contractors make in response to extreme heat, likely reflecting their greater need to manage heat stress.

Work Schedule Adjustment. Contractors and non-contractors adjust their daily work schedules differently in response to high temperatures. As shown in Figure 10, contractors are less likely to undertake any driving tasks on hotter days, whereas non-contractors' daily driving participation is largely inelastic with respect to temperature. In addition, conditional on working, contractors are substantially more likely than non-contractors to start work later than their usual schedule on hot days. Together, these patterns indicate that contractors face fewer constraints on labor supply and can more readily adjust their daily schedules to mitigate exposure to extreme heat.

5.5.2 Performance Outcome of Heterogeneous Adaptations

The differential adaptation responses between these two types of drivers can translate into systematically different performance outcomes. Figure 11 presents the heterogeneous effects of temperature on alarm intensity across contractors and non-contractors. Contractors bear the most severe impacts of high temperatures, as evidenced by their significantly higher alarm intensity compared to employed drivers. An additional hour of exposure to temperatures above 33°C increases the number of alarms per 100 km of driving by 0.6 for contractors – almost three times that of non-contractors. The results suggest that

contractors are much more likely to have dangerous driving behaviors under extreme heat, relative to employed drivers.

The heightened risk among contractors during extreme heat is accompanied by larger declines in productivity. To investigate how contractors and non-contractors adjust their driving activities under heat stress, Figure D10 examines the effects of temperature on driving intensity and speed. Contractors experience a sharper reduction in both driving distance and hours compared to non-contractors during hot temperatures. Additionally, contractors exhibit a more pronounced decrease in mean and maximum speeds. These results point to larger productivity losses among contractors when exposed to extreme heat.

5.6 Robustness Checks and Alternative Explanations

Alternative Model Specifications. Our results are robust to alternative measures of temperature exposure and model specifications, as presented in Figure D11. In Panel (a), we re-estimate Equation 1 using binary indicators for whether the daily average temperature exposure falls within specific ranges as the temperature variables on the right-hand side. Panel (b) measures temperature exposure by calculating the driving distance (in kilometers) with temperatures falling into each range. Panel (c) measures alarm intensity using the total number of alarms per hour of driving. In Panel (d), we re-estimate Equation 1 by replacing date fixed effects with various combinations of alternative time fixed effects. Panel (e) applies a Poisson regression model, while Panel (f) estimates an unweighted version of Equation 1. Similarly, as shown in Figure D12, we find consistent results when using the total number of alarms as the dependent variable while controlling for driving distance or hours.

Controlling for Additional Meteorological Conditions. Our findings remain robust when additional meteorological variables are included as controls. Figure D13 presents the estimation results. First, humidity conditions, which are correlated with temperature, may influence drivers' behaviors. Since the ERA5 dataset does not provide humidity information, we use two proxies instead: relative humidity and dew point temperature. Second, cloud conditions can influence apparent temperature and driving behavior. We account for this by including the proportion of the area covered by clouds as a control variable. Third, we incorporate daily average UV radiation as an additional control to account for its potential effects on driving visibility under intense sunlight.

Controlling for Additional Road Conditions. Drivers on different trips may encounter varying road conditions, which could confound the analysis. To address these concerns, our main model specification includes controls for elevation, slope, and the share of water areas. In Figure D14, we show that our coefficient estimates remain largely unchanged when additional road condition controls are included. First, we control for the fraction of areas covered by vegetation, such as trees or woodland. Second, we account for the density of leaf area in a given ground area. Third, for each route a driver follows in a day, we create binary indicators for whether the route passes through specific counties and include these indicators as additional controls in the regression. This approach allows us to flexibly account for unobserved county-level differences, such as urbanization levels, road quality, traffic regulations, or regional policies, that may influence driving behavior.

Controlling for Traffic Conditions. Temperature may also affect traffic conditions, such as causing congestion, which could influence driving behavior and safety outcomes. To address this potential confounding factor, we conduct robustness checks using different proxies for traffic conditions. The results are presented in Figure D15. First, we incorporate mean driving speed as a control variable (Panel a). Since higher traffic congestion often leads to lower speeds, controlling for mean speed helps account for variations in traffic intensity that might confound the relationship between temperature and alarm intensity. Second, we focus on non-blind-spot alarms while controlling for blind-spot alarms (Panel b). Since blind-spot alarms mainly capture the surrounding conditions, such as nearby vehicles or pedestrians, this approach helps isolate the effect of temperature on alarms that are less directly influenced by external traffic factors. Third, we adopt a more conservative strategy by restricting the analysis to alarms related to inside conditions while controlling for alarms related to outside conditions (Panel c). Alarms tied to outside conditions, such as collisions or following too closely, are more likely to reflect external traffic dynamics. Controlling for these outside alarms further isolates the direct impact of temperature on drivers' internal behaviors. Across all three approaches, our results remain robust, with coefficient estimates mostly unchanged.

Ruling Out Alternative Explanations for Contractor Heterogeneity. We conduct comprehensive analyses to show that the heterogeneity between contractors vs non-contractors cannot be explained by differences in driver characteristics, exposure to diverse weather conditions, or transport categories. We start with comparing contractors to non-contractors in terms of their driving characteristics and exposure to various environmental conditions. Figure D16 confirms that both groups have a similar distribution of temperature exposure

over the sample period. Table D1 provides a balance check between companies operating as contractors and those operating as non-contractors. Across most dimensions, such as resting behavior and weather exposure, the two groups exhibit comparable patterns. Only a few notable differences emerge: on average, contractor companies are less likely to engage in passenger transportation, and drivers associated with these companies tend to work for slightly longer distances.

Next, we demonstrate that the heterogeneous responses between contractors and non-contractors are not driven by the potential differences in transport categories. Figure D17 presents the effect of temperature by transport category, separately for contractors and non-contractors. The results consistently show that contractors trigger more alarms during hot temperatures compared to non-contractors, even when focusing specifically on drivers involved in non-passenger transportation or transporting non-hazardous cargo. For the transportation of passengers or hazardous cargo, we do not observe meaningful differences between contractors and non-contractors, and the coefficients are imprecisely estimated, likely due to the much smaller sample size.[29]

Further, we provide evidence that differences in drivers' skill levels or risk preferences do not explain the heterogeneous responses between contractors and non-contractors. To proxy for baseline characteristics, we calculate each driver's average alarm intensity, average speed, and number of short rests per 100 km of driving on mild-temperature days (i.e., $\leq$24°C). We then augment the regression model by adding interaction terms between the full set of temperature exposure variables and these demeaned baseline performance measures. These interactions flexibly capture variation in temperature responses attributable to drivers' personal characteristics. Figure D18 presents the coefficient estimates for the temperature exposure variables themselves. The results confirm that, even after accounting for baseline performance differences, contractors remain significantly more sensitive to high temperatures than non-contractors.

5.7 Back-of-the-Envelope Calculation on Damage from Heat Exposure

How much is the cost of heat-induced dangerous driving behaviors? To quantify the economic losses, we first link dangerous driving behaviors to the likelihood of traffic accidents. Then, we estimate the monetary losses associated with the additional fatalities, injuries, and property damage resulting from these accidents.

[29]Contractor information is available for 639,553 out of 2,224,116 observations. Among these, only 2% are engaged in hazardous-cargo or passenger transportation.

Truck Drivers' Behaviors and Accidents. To map the occurrence of dangerous driving behaviors to traffic accidents, we model the number of accidents (within a specific time interval), N, using a Poisson distribution, i.e., $N \sim \text{Poisson}(\lambda)$.[30] We assume the expected number of accidents λ is

$$\lambda = \exp(\beta_0 + \underbrace{\beta_1 \cdot \ln X}_{\text{impact of dangerous driving behaviors}})$$

where X is the number of dangerous driving behaviors. β_1 is the key elasticity parameter that captures the proportional change in the number of accidents with respect to changes in dangerous driving behaviors. β_0 is a normalizer to adjust based on the time interval.

We calibrate this elasticity leveraging data from the 100-Car Naturalistic Driving Study (Dingus et al., 2006).[31] This study collects large-scale naturalistic driving data from approximately 100 vehicles, each equipped with a suite of sensors and cameras. The publicly available dataset includes detailed information on drivers' behaviors and crash incidents. We identify instances of dangerous driving behavior and aggregate the data at the vehicle-driver level. Using this dataset, we estimate the following Poisson regression model:

$$\lambda_i = \exp(\beta_0 + \beta_1 \ln X_i + \gamma \mathbf{Z}_i) + \varepsilon_i, \tag{2}$$

where λ_i is the number of accidents, X_i is the number of dangerous driving behaviors, and $\mathbf{Z}$ is a set of driver i's characteristics, including gender and age. Table D3 presents the estimation results. We find $\beta_1 = 0.808$, indicating that a 1% increase in dangerous driving behaviors is associated with a 0.808% increase in the expected number of accidents.

Based on estimation from our preferred specification, an extra hour with temperature exposure above 33°C leads to a 3% increase in the incidence of dangerous driving behaviors (i.e., $\Delta \ln X = 3\%$). Therefore, applying the estimated elasticity $\beta_1 = 0.808$, the expected number of accidents increases by $\beta_1 \cdot \Delta \ln X = 0.808 \times 3\% = 2.4\%$. This implies that one extra hour of extreme temperature exposure can result in a 2.4% rise in the number of truck crashes.

[30] The probability density function is $P(N = n) = \frac{\lambda^n e^{-\lambda}}{n!}$, $n = 1, 2, 3....$

[31] Although our driving monitoring sensor data provides detailed records of warnings, it lacks information on associated traffic accidents. Hence, we leverage the 100-Car dataset (Custer, 2018), constructed by Dingus et al. (2006), which, to our knowledge, is the best available data we can use to estimate the relationship between dangerous driving behavior and accidents.

Monetary Loss from Truck Accidents. To put the increased crashes in value terms, we bring in additional parameters calibrated from various sources as listed in Table D4. When data from both China and the US are available, we prioritize Chinese data for the calculation; otherwise, US data are used. All numbers are yearly basis. Since our main specification employs daily-level analysis, we normalize the calculations to a daily basis. The underlying assumption is that the adverse effects of extreme heat on drivers are short-term and do not accumulate throughout the day.[32] The detailed formulas used for these calculations are provided in Appendix B.

Based on our calculations shown in Panel B of Table D2, the total monetary loss associated with truck accidents in China amounts to approximately 31 million USD per day. Consequently, an additional hour of temperature exposure above 33°C for all truck drivers in China is expected to increase this loss by 0.77 million USD. Of this amount, approximately 0.17 million USD (22%) is attributed to the direct costs borne by truck drivers, while the remaining 0.6 million USD (78%) stems from the negative externalities imposed on other road users.

6 A Model of Steering Adaptation

This section develops a simple model of firm-steered adaptation. The model is designed to rationalize four empirical findings. First, workers adapt more as heat exposure rises. Second, employee drivers and contractors adapt along different margins. Third, employee drivers are less adversely affected by extreme heat, despite the presence of moral hazard under firm cost-sharing. Fourth, the employee-contractor gap widens with temperature. The model formalizes how firm involvement in adaptation creates a trade-off between improved risk sharing and moral hazard, and it provides a framework for quantifying how much firm steering mitigates the negative consequences of heat.

6.1 Setup and decision rules

Consider a driver facing heat exposure T and deciding whether to adopt a given adaptation method, such as air conditioning, rest-taking, or work rescheduling. Let B denote the true

[32] This assumption would generate conservative estimates. If cumulative effects were considered, the calculated monetary loss would be larger.

net marginal benefit of adaptation, where

$$B \sim F_B(\cdot \mid T), \qquad \mathbb{E}[B \mid T] \text{ increasing in } T.$$

The object B captures the performance value of adaptation, for example through lower accident risk or improved productivity. Let $c > 0$ denote the direct marginal cost of adaptation. For air conditioning, c may represent additional fuel costs; for resting or schedule adjustment, it may capture the opportunity cost of forgone output.

In addition, workers face an idiosyncratic private component

$$v \sim H_v(\cdot \mid T).$$

The term v captures private value or private cost that is not fully contractible. Positive values of v may reflect private motives that encourage excessive adaptation, such as shirking or using heat as a pretext for reducing effort. Negative values of v may instead reflect inertia, inattention, or underestimation of heat-related risk. We interpret v as the private wedge between the worker's perceived payoff from adaptation and the firm's objective payoff.

The key distinction between contractors and employee drivers is cost-sharing. Let $\theta \in (0, 1]$ denote the share of adaptation benefits and costs borne by the worker. When $\theta = 1$, the worker fully internalizes the consequences of adaptation, corresponding to the contractor benchmark. When $\theta < 1$, part of the consequences is shared with the firm, corresponding to employee drivers. In addition, the firm may impose an implicit wedge $\tau^E(T)$ that either encourages adaptation ($\tau^E < 0$) or discourages it ($\tau^E > 0$).

The adaptation decision rules are therefore

$$\begin{aligned}
\text{First-best:} \quad & B \geq c, && (3)\\
\text{Contractor:} \quad & B + v \geq c, && (4)\\
\text{Employee (no steering):} \quad & \theta B + v \geq c, && (5)\\
\text{Employee:} \quad & \theta B + v - \tau^E(T) \geq c. && (6)
\end{aligned}$$

Equation (4) shows that contractors choose adaptation based on the sum of the true marginal benefit B and the private component v, because they bear the direct consequences of their choices. Equation (5) highlights the moral-hazard channel for employee drivers: since they internalize only a fraction θ of the true return to adaptation, private consid-

erations receive greater weight in the adaptation decision. Equation (6) introduces firm steering through $\tau^E(T)$, which summarizes the firm's effort to correct workers' private bias.

6.2 The firm's problem

The firm chooses $\tau^E(T)$ to maximize its expected payoff from employee adaptation. Conditional on heat exposure T, the firm's expected payoff is

$$\Pi(\tau, T) = \mathbb{E}\left[(1-\theta)(B-c)\cdot \mathbf{1}\{\theta B + v - \tau \geq c\} \mid T\right].$$

Equivalently,

$$\Pi(\tau, T) = \int_{-\infty}^{+\infty} \int_{\tau-\theta(B-c)}^{+\infty} (1-\theta)(B-c)\, dH_v\, dF_B.$$

The firm solves

$$\tau^E(T) \in \arg\max_{\tau(T)} \Pi(\tau(T), T).$$

The first-order condition takes the average marginal bias form:

$$\tau^E(T) = \mathbb{E}\Big[v \,\Big|\, v + \theta(B-c) - \tau^E(T) = 0,\ T\Big]. \tag{7}$$

Equation (7) implies that the firm sets the wedge to offset the average private bias among marginal workers. If marginal workers have positive private bias, the firm optimally raises the effective cost of adaptation. If marginal workers instead under-adapt because of negative private bias, the firm subsidizes or facilitates adaptation.

This setup makes clear why firm involvement can steer adaptation in both directions. When workers under-adapt because they do not fully internalize the benefits of adaptation, the firm has an incentive to encourage adaptation. When workers overuse adaptation along dimensions that are privately beneficial but costly to the firm, the firm has an incentive to restrict those margins. The model therefore nests risk sharing and moral hazard in a unified way.

6.3 Illustration of the model mechanism

It is useful to begin with the model's economic logic. Suppose $\theta < 1$, $\mathbb{E}[B] = c$, and $\mathbb{E}[v] < 0$. In this case, workers under-adapt relative to the first best. Intuitively, even if

the average true marginal benefit of adaptation equals its marginal cost, private frictions such as inattention, inertia, or underestimation of heat risk imply that contractors adopt too little adaptation. Employee drivers, in the absence of firm steering, adopt even less, because they internalize only a fraction θ of the true return. As a result,

$$Q^{FB} > Q^{C} \geq Q^{E}(\tau^{E} = 0),$$

where Q^{FB} denotes the first-best adaptation rate, Q^{C} the contractor adaptation rate, and $Q^{E}(\tau^{E} = 0)$ the employee adaptation rate without firm intervention.

The firm responds by choosing a wedge τ^{E} to shift employee behavior toward the firm's preferred adaptation level. The optimal wedge satisfies

$$\tau^{E} = \mathbb{E}\left[v \mid \theta B + v = \theta c + \tau^{E}\right].$$

When the average private bias is negative, the optimal wedge is negative: the firm effectively lowers the cost of adaptation, either by directly covering part of the cost or by facilitating the use of the adaptation margin. In this case, firm steering raises employee adaptation from $Q^{E}(\tau^{E} = 0)$ toward the first-best benchmark.

Figure D19 illustrates this logic. The first figure shows why, absent firm steering, adaptation is lower for employee drivers than for contractors when workers do not fully internalize the returns to adaptation and the average private wedge is negative. The second figure shows how the firm uses the wedge τ^{E} to shift employee behavior toward the first-best level.

6.4 Identification and Estimation

The key latent objects in the model are the temperature-dependent distributions of the true marginal benefit of adaptation, $F_B(\cdot \mid T)$, and the private component, $H_v(\cdot \mid T)$. We do not observe either object directly, nor do we observe the firm's wedge $\tau^{E}(T)$. Identification instead comes from comparing adaptation responses of employee and contractor drivers across temperatures. Under the maintained assumption that the firm chooses $\tau^{E}(T)$ according to the average marginal bias rule in (7), employee behavior is informative about how the true value of adaptation changes with temperature, because firm steering offsets the average private bias of marginal workers. Contractor behavior, by contrast, reflects both the true marginal benefit and the private component, since contractors choose adaptation based on $B + v$ without firm intervention. The gap between employee and contractor

responses therefore identifies how the private component varies with temperature.

Figure D20 illustrates this logic. As temperature rises from T_0 to T_1, the employee response traces out how $F_B(\cdot \mid T)$ shifts with heat exposure, while the contractor response combines this movement with changes in $H_v(\cdot \mid T)$. The evolution of the employee-contractor gap across temperatures therefore reveals how private distortions change with heat exposure. We implement this idea separately for the three main adaptation margins in the data—air conditioning, resting, and labor supply—by matching model-implied and empirical temperature-response profiles for employee and contractor drivers. We then map the estimated adaptation responses into performance outcomes, such as dangerous driving behaviors, through margin-specific outcome weights. The details of the parameterization, moment conditions, and estimation procedure are described in Appendix C.

Table 3 summarizes the estimates. Two results stand out. First, for resting and labor supply, the average private component becomes more positive as temperature rises, indicating that moral hazard becomes increasingly important for these margins under extreme heat. By contrast, the private component is much less important for air conditioning. Second, the estimated outcome weights imply that air conditioning is the most effective adaptation margin, whereas resting and labor supply adjustment are less effective at offsetting the negative performance consequences of heat. Taken together, the estimates suggest that the main difference between employee and contractor drivers is not whether they adapt at all, but how they adapt and how firms shape these choices: air conditioning is both the most effective and the least distortion-prone margin, while resting and labor supply adjustments are more exposed to private incentives and hence more susceptible to moral hazard.

6.5 Counterfactual Decomposition

We use the estimated model to decompose the observed employee-contractor gap into a moral-hazard component and a steering component. The key counterfactual asks what would happen if employee drivers faced the same cost-sharing arrangement as in the data, but without firm steering. Comparing this benchmark to the observed employee outcome isolates the role of firm steering. Comparing it to the contractor benchmark isolates the effect of moral hazard generated by cost-sharing.

Figure 12 reports the decomposition for dangerous driving behaviors. The first result is that moral hazard works in the expected direction: holding firm steering fixed, partial cost-sharing would lead employee drivers to perform worse than contractors along some

adaptation margins, because workers internalize only part of the true return to adaptation. However, the second and quantitatively more important result is that the steering effect dominates. Once firms optimally adjust the wedge, employee drivers perform substantially better than they would under cost-sharing alone, and the observed employee-contractor difference is driven mainly by this endogenous steering response.

This decomposition sharpens the interpretation of the reduced-form evidence. Employee drivers are not less affected by heat simply because their costs are shared. If anything, cost-sharing alone would create additional distortions through moral hazard. What reduces their heat-induced performance losses is that firms steer them toward adaptation margins that are more effective and less prone to misuse, especially air conditioning, while discouraging margins such as excessive rest-taking or labor supply reductions. In this sense, the model attributes the smaller employee effect primarily to firm steering rather than to passive insurance.

More broadly, the decomposition highlights the central trade-off in the paper. Firm involvement in adaptation is not unambiguously beneficial, because it creates room for moral hazard whenever workers do not fully internalize the consequences of their choices. At the same time, firm steering can substantially offset these distortions and improve adaptation efficiency. In our setting, the second force dominates the first.

7 Conclusion

This paper studies how extreme heat affects worker performance and adaptation, and how firms shape these responses through labor contracts and cost-sharing arrangements. Using high-frequency GPS records, AI-based driver monitoring data, and satellite weather data from China's heavy-duty trucking industry, we show that extreme heat worsens driver performance: exposure to temperatures above 33°C increases dangerous driving behaviors and reduces daily working time and delivery distance.

We also show that adaptation is both observable and contract-sensitive. Drivers respond to heat by increasing air conditioning usage, taking more frequent and longer rests, and adjusting work schedules. These responses differ sharply across labor contracts. Owner-operators, who bear operating costs directly, are less likely to adapt through air conditioning and rely more on rest and schedule adjustment. Employee drivers, by contrast, adapt more through air conditioning and less through margins that are harder for firms to verify or manage. Consistent with these differences, the adverse effects of heat

are substantially larger for owner-operators than for employee drivers.

To interpret these patterns, we develop a model of firm-steered adaptation in which firm involvement creates a trade-off between improved risk sharing and moral hazard. The model implies that employee behavior reflects both partial cost sharing and endogenous firm steering. In the quantitative analysis, steering more than offsets the distortions that would arise from moral hazard alone and accounts for a substantial share of the observed employee-contractor gap in heat-induced dangerous driving. More broadly, the results imply that adaptation to climate risk depends not only on exposure, but also on organizational form and incentive design.

These findings have two main implications. First, workplace heat policy should account for differences in labor contracts, since workers who bear operating costs directly face stronger barriers to effective adaptation. Second, in settings where unsafe performance generates externalities, private adaptation is unlikely to be socially efficient. Policies that improve adaptation through verifiable and incentive-compatible margins may therefore yield benefits that extend beyond workers themselves.

Our analysis is specific to heavy-duty trucking in Guangdong, but the underlying mechanism is broader. Similar trade-offs between cost sharing, private incentives, and firm steering are likely to arise in other high-risk sectors in which adaptation is costly, imperfectly contractible, and consequential for third parties.

References

Adhvaryu, Achyuta, Namrata Kala, and Anant Nyshadham. 2022. "Management and shocks to worker productivity." *Journal of Political Economy*, 130(1): 1–47.

Alder, Simon, Michael Zheng Song, and Zhitao Zhu. 2023. "On (Un) Congested Roads: A Quantitative Analysis of Infrastructure Investment Efficiency using Truck GPS Data." Working Paper.

Anderson, Michael L, and Maximilian Auffhammer. 2014. "Pounds that kill: The external costs of vehicle weight." *Review of Economic Studies*, 81(2): 535–571.

Baker, George P., and Thomas N. Hubbard. 2003. "Make Versus Buy in Trucking: Asset Ownership, Job Design, and Information." *American Economic Review*, 93(3): 551–572.

Baker, George P., and Thomas N. Hubbard. 2004. "Contractibility and Asset Ownership: On-Board Computers and Governance in U.S. Trucking." *Quarterly Journal of Economics*, 119(4): 1443–1479.

Balboni, Clare, Johannes Boehm, and Mazhar Waseem. 2024. "Firm Adaptation in Production Networks: Evidence from Extreme Weather Events in Pakistan." Working Paper.

Barnwal, Prabhat, Jonathan I Dingel, Daniil Iurchenko, Pravin Krishna, and Eva Van Leemput. 2024. "Internal Trade Barriers in India."

Barreca, Alan, Karen Clay, Olivier Deschenes, Michael Greenstone, and Joseph S Shapiro. 2016. "Adapting to climate change: The remarkable decline in the US temperature-mortality relationship over the twentieth century." *The journal of political economy*, 124(1): 105–159.

Baylis, P W, and J Boomhower. 2021. "Mandated vs. voluntary adaptation to natural disasters: the case of US wildfires."

Burchardi, Konrad B., Selim Gulesci, Benedetta Lerva, and Munshi Sulaiman. 2019. "Moral Hazard: Experimental Evidence from Tenancy Contracts." *Quarterly Journal of Economics*, 134(1): 281–347.

Burke, Marshall, and Kyle Emerick. 2016. "Adaptation to climate change: Evidence from US agriculture." *American Economic Journal. Economic Policy*, 8(3): 106–140.

Cao, Chaoji, Xinke Song, Wenjia Cai, Yichao Li, Jianhui Cong, Xueying Yu, Mengzhao Gao, and Can Wang. 2023. "Estimating the value of a statistical life in China: A contingent valuation study in six representative cities." *Chinese Journal of Population, Resources and Environment*, 21(4): 269–278.

Carson, Richard, and Alex Chu Yu. 2024. "Exploring the Sources and Nature of Temperature Measurement Error in Estimating Climate Related Impacts." Working Paper.

Chen, Jingjing, Wei Chen, Ernest Liu, Jie Luo, and Zheng Song. 2025. "The economic cost of locking down like china: Evidence from city-to-city truck flows." *Journal of Urban Economics*, 145: 103729.

Cui, Xiaomeng. 2020. "Climate change and adaptation in agriculture: Evidence

from US cropping patterns." *Journal of environmental economics and management*, 101(102306): 102306.

Cui, Xiaomeng, and Wei Xie. 2022. "Adapting agriculture to climate change through growing season adjustments: Evidence from corn in China." *American journal of agricultural economics*, 104(1): 249–272.

Cui, Xiaomeng, Bulat Gafarov, Dalia Ghanem, and Todd Kuffner. 2024. "On model selection criteria for climate change impact studies." *Journal of Econometrics*, 239(1): 105511.

Custer, Kenny. 2018. "100-Car Data." Available at http://dx.doi.org/10.15787/VTT1/CEU6RB.

Davis, Lucas, Paul Gertler, Stephen Jarvis, and Catherine Wolfram. 2021. "Air conditioning and global inequality." *Global environmental change: human and policy dimensions*, 69(102299): 102299.

Deschênes, Olivier, and Michael Greenstone. 2011. "Climate Change, Mortality, and Adaptation: Evidence from Annual Fluctuations in Weather in the US." *American Economic Journal: Applied Economics*, 3(4): 152–185.

Dey, Matthew, and Susan Houseman. 2025. "The Rise of the Contract Workforce in US Manufacturing." In *The Changing Nature of Work*. Chapter 7. University of Chicago Press. NBER Chapter.

Dingus, T A, S G Klauer, V L Neale, A Petersen, S E Lee, J Sudweeks, M A Perez, J Hankey, D Ramsey, S Gupta, C Bucher, Z R Doerzaph, J Jermeland, and R R Knipling. 2006. "The 100-car naturalistic driving study, phase II - results of the 100-car field experiment."

Drescher, Katharina, and Benedikt Janzen. 2025. "When weather wounds workers: The impact of temperature on workplace accidents." *Journal of public economics*, 241(105258): 105258.

Farrington, Rob, and John Rugh. 2000. "Impact of vehicle air-conditioning on fuel economy, tailpipe emissions, and electric vehicle range." National Renewable Energy Lab.(NREL), Golden, CO (United States).

Filomena, Mattia, and Matteo Picchio. 2024. "Unsafe temperatures, unsafe jobs: The impact of weather conditions on work-related injuries." *Journal of Economic Behavior & Organization*, 224: 851–875.

Garg, Teevrat, Maulik Jagnani, and Vis Taraz. 2020. "Temperature and human capital in India." *Journal of the Association of Environmental and Resource Economists*, 7(6): 1113–1150.

Ghanem, Dalia, and Aaron Smith. 2021. "What are the benefits of high-frequency data for fixed effects panel models?" *Journal of the Association of Environmental and Resource Economists*, 8(2): 199–234.

Graff Zivin, Joshua, and Matthew Neidell. 2014. "Temperature and the allocation of time: Implications for climate change." *Journal of labor economics*, 32(1): 1–26.

Grover, Arti, and Matthew E Kahn. 2024. "Firm Adaptation to Climate Change." National Bureau of Economic Research w32848.

Heutel, Garth, Nolan H Miller, and David Molitor. 2021. "Adaptation and the mortality effects of temperature across U.s. climate regions." *The Review of Economics and Statistics*, 103(4): 740–753.

Hubbard, Thomas N. 2003. "Information, Decisions, and Productivity: On-Board Computers and Capacity Utilization in Trucking." *American Economic Review*, 93(4): 1328–1353.

Huff, Shean, Brian West, and John Thomas. 2013. "Effects of air conditioner use on real-world fuel economy." SAE Technical Paper.

Ireland, Andrew, David Johnston, and Rachel Knott. 2023. "Heat and worker health." *Journal of health economics*, 91: 102800.

Kelley, Erin M., Gregory Lane, and David Schönholzer. 2024. "Monitoring in Small Firms: Experimental Evidence from Kenyan Public Transit." *American Economic Review*, 114(10): 3119–3160.

Laffont, Jean-Jacques, and Mohamed Salah Matoussi. 1995. "Moral Hazard, Financial Constraints and Sharecropping in El Oulja." *Review of Economic Studies*, 62(3): 381–399.

Leard, Benjamin, and Kevin Roth. 2019. "Voluntary exposure benefits and the costs of climate change." *Journal of the Association of Environmental and Resource Economists*, 6(1): 151–185.

Lee, Jungwoo, Jaeheun Kim, Jungseo Park, and Choongsik Bae. 2013. "Effect of the air-conditioning system on the fuel economy in a gasoline engine vehicle." *Proceedings of the Institution of Mechanical Engineers, Part D: Journal of Automobile Engineering*, 227(1): 66–77.

Li, Shanjun. 2012. "Traffic safety and vehicle choice: quantifying the effects of the 'arms race'on American roads." *Journal of Applied Econometrics*, 27(1): 34–62.

Pankratz, Nora M C, and Christoph M Schiller. 2024. "Climate Change and Adaptation in Global Supply-Chain Networks." *The Review of Financial Studies*, 37(6): 1729–1777.

Park, Jisung, Nora Pankratz, and Arnold Behrer. 2021. "Temperature, workplace safety, and labor market inequality."

Park, R Jisung, Joshua Goodman, Michael Hurwitz, and Jonathan Smith. 2020. "Heat and Learning." *American Economic Journal: Economic Policy*, 12(2): 306–339.

Patel, Dev. 2024. "Learning About a Warming World: Attention and Adaptation in Agriculture." Working Paper.

Rode, Ashwin, Rachel E Baker, Tamma Carleton, Anthony D'Agostino, Michael Delgado, Timothy Foreman, Diana R Gergel, Michael Greenstone, Trevor Houser, Solomon Hsiang, Andrew Hultgren, Amir Jina, Robert E Kopp, Steven B Malevich, Kelly McCusker, Ishan Nath, Matthew Pecenco, James Rising, and Jiacan Yuan. 2022. "Labor disutility in a warmer world: The impact of climate change on the global workforce." *SSRN Electronic Journal*.

Rugh, John, Valerie Hovland, and Stephen O Andersen. 2004. "Significant fuel savings and emission reductions by improving vehicle air conditioning." *Mobile Air Conditioning Summit, Washington, DC*.

Sexton, Steven, Zhenxuan Wang, and Jamie T Mullins. 2022. "Heat adaptation and human performance in a warming climate." *Journal of the Association of Environmental and Resource Economists*, 9(1): 141–163.

Somanathan, Eswaran, Rohini Somanathan, Anant Sudarshan, and Meenu Tewari. 2021. "The impact of temperature on productivity and labor supply: Evidence from Indian manufacturing." *Journal of Political Economy*, 129(6): 1797–1827.

Tan, Hong, Fuquan Zhao, Han Hao, and Zongwei Liu. 2020. "Cost analysis of road traffic crashes in China." *International journal of injury control and safety promotion*, 27(3): 385–391.

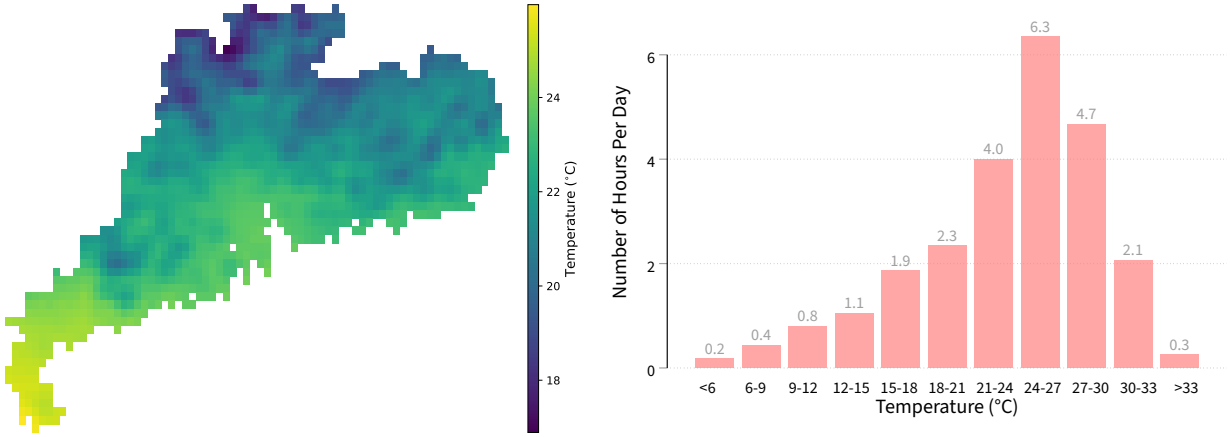
Wu, Shenyu, Li Feng, Sina Changizian, Mehrdad Raeesi, and Hamid Aiedi. 2022. "Analysis of air conditioning system impact on a fuel cell vehicle performance based on a realistic model under actual urban conditions." *International Journal of Hydrogen Energy*, 47(62): 25899–25912.

Xia, Fan, Ximeng Cheng, Zhen Lei, Jintao Xu, Yu Liu, Yingxin Zhang, and Qinghong Zhang. 2023. "Heterogeneous impacts of local traffic congestion on local air pollution within a city: Utilizing taxi trajectory data." *Journal of Environmental Economics and Management*, 122: 102896.

Yu, Ao. 2024. "New Estimates of the Value Per Statistical Life in China: Evidence from the Automobile Market."

Zhang, Peng, Olivier Deschenes, Kyle Meng, and Junjie Zhang. 2018. "Temperature effects on productivity and factor reallocation: Evidence from a half million chinese manufacturing plants." *Journal of environmental economics and management*, 88: 1–17.

Figures and Tables



(a) Spatial Distribution of Average Temperature (b) Distribution of Temperature Exposure within a Day

Figure 1: Temperature Distribution

Notes: Panel (a) displays the mean daily average temperature over the sample period (March 2023 - June 2024) for ERA5-Land grids located within Guangdong province. Panel (b) illustrates the average number of hours per day that drivers are exposed to temperatures within specific ranges.

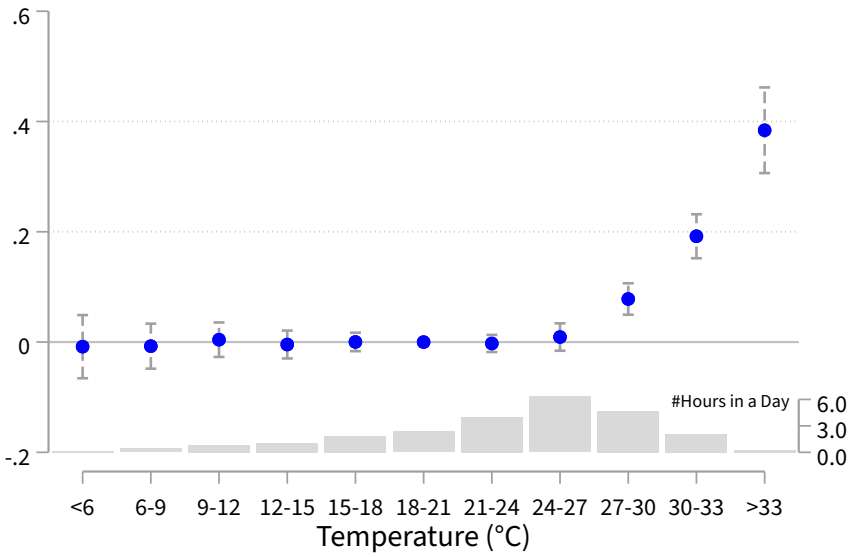
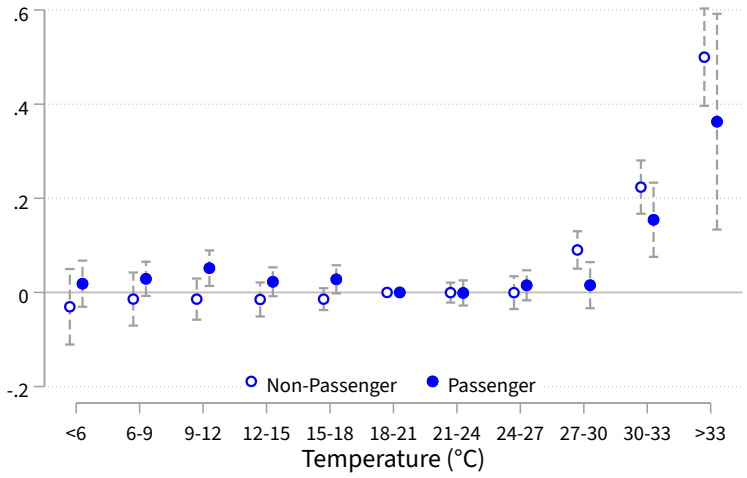
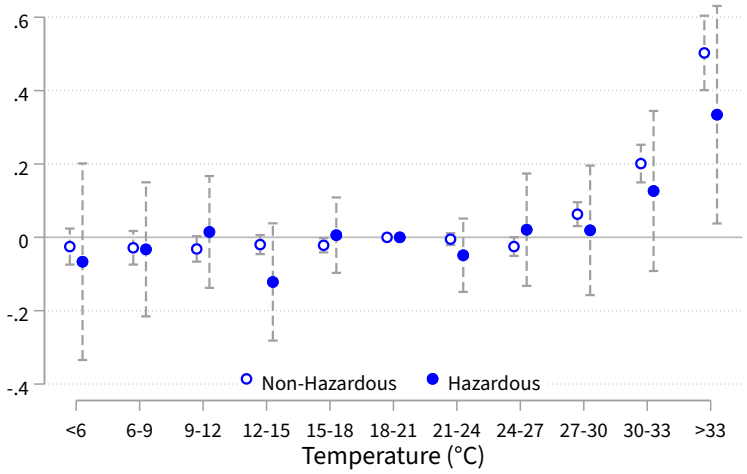


Figure 2: Effect of Heat on All Alarms

Notes: This figure displays the estimated effects of hourly temperature exposure on the total number of alarms per 100 km of driving. The blue dots represent the point estimates, while the gray vertical caps indicate the corresponding 95% confidence intervals. The regression model includes control variables such as other weather conditions, air quality, and geographic characteristics, along with vehicle fixed effects and date fixed effects. The temperature range of 18–21°C is the omitted category, serving as the reference group for comparison. Standard errors are clustered at the vehicle level. The gray bars at the bottom plot the average number of hours within a day with exposure to temperature in each bin.



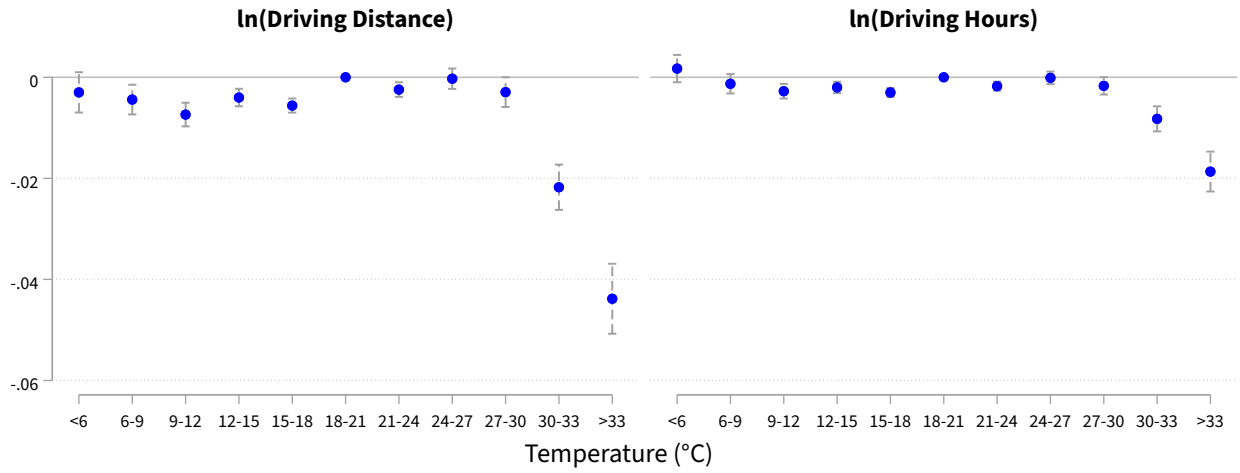
(a) Passenger vs Non-Passenger Transportation



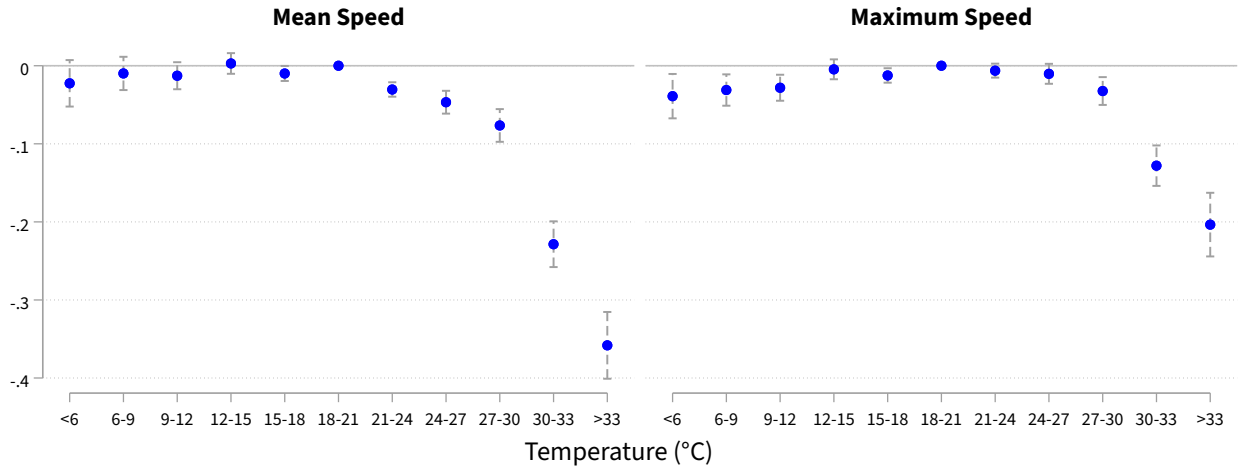
(b) Hazardous vs Non-Hazardous Cargo

Figure 3: Heterogeneity by Transport Category

Notes: This figure presents the estimated effects of hourly temperature exposure on the number of alarms per 100 km of driving, analyzed separately by transport category. For a subsample of vehicles whose company information is available, we classify them into different groups based on their company's business scope. In Panel (a), vehicles are classified into two groups: those engaging in passenger transportation (blue dots) and those not (white dots). In Panel (b), vehicles are categorized as either transporting hazardous cargo (blue dots) or non-hazardous cargo (white dots). The dots represent the point estimates, while the gray vertical caps indicate the corresponding 95% confidence intervals. Each panel is a separately estimated regression model that includes control variables such as other weather conditions, air quality, and geographic characteristics, along with vehicle fixed effects and date fixed effects. The temperature range of 18–21°C is the omitted category, serving as the reference group for comparison. Standard errors are clustered at the vehicle level.



(a) Driving Distance and Hours



(b) Driving Speed

Figure 4: Effect of Heat on Individual Productivity: Driving Intensity and Speed

Notes: This figure displays the estimated effects of hourly temperature exposure on driving distance, driving hours, mean speed, and maximum speed. Panel (a) presents logarithm of driving distance (km) and driving hours. Panel (b) presents mean and maximum speed (km/h). The blue dots represent the point estimates, while the gray vertical caps indicate the corresponding 95% confidence intervals. Regression models include control variables such as other weather conditions, air quality, and geographic characteristics, along with vehicle fixed effects and date fixed effects. The temperature range of 18–21°C is the omitted category, serving as the reference group for comparison. Standard errors are clustered at the vehicle level.

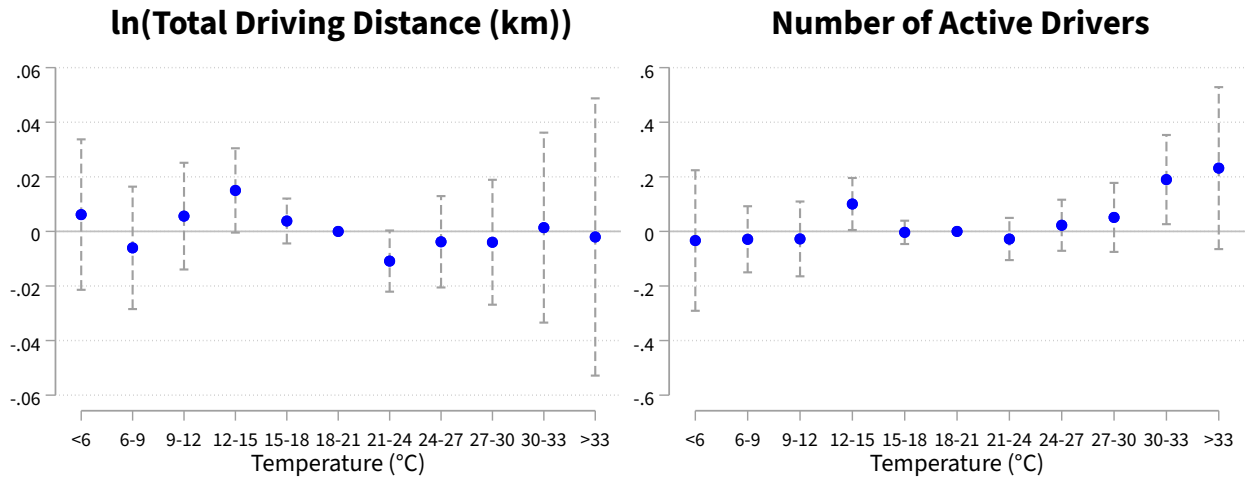


Figure 5: Effect of Heat on Transportation Companies' Productivity and Response

Notes: This figure presents the estimated effects of temperature on transportation companies' operation. We aggregate the data to the company-by-day level and measure the average distribution of temperature exposure for all drivers working for a company in a day. In the left panel, the outcome variable is the logarithm of total driving distance for a company's transportation tasks in a day. In the right panel, the outcome variable is the number of active drivers working in a day. The blue dots represent the point estimates, while the gray vertical caps indicate the corresponding 95% confidence intervals. The regression model includes control variables such as other weather conditions, air quality, and geographic characteristics, along with company fixed effects and date fixed effects. The temperature range of 18–21°C is the omitted category, serving as the reference group for comparison. Standard errors are clustered at the company level.

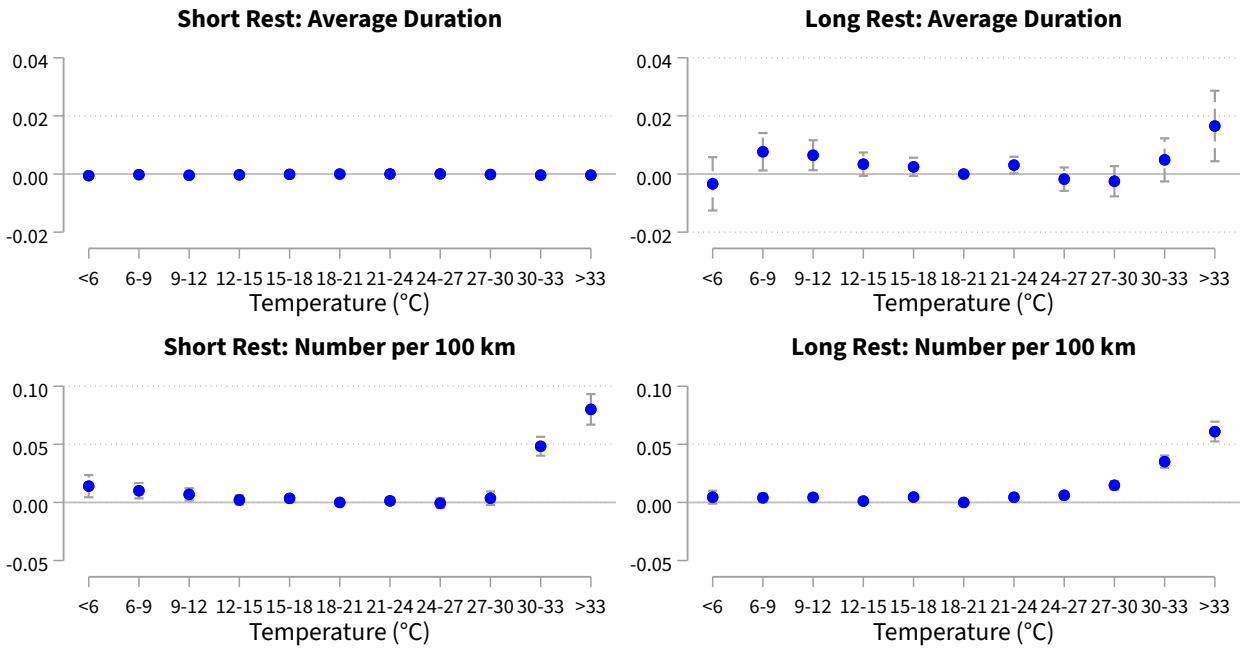
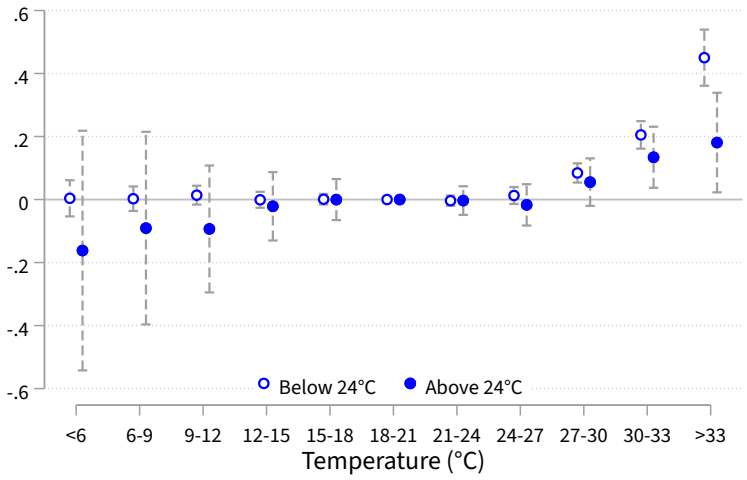
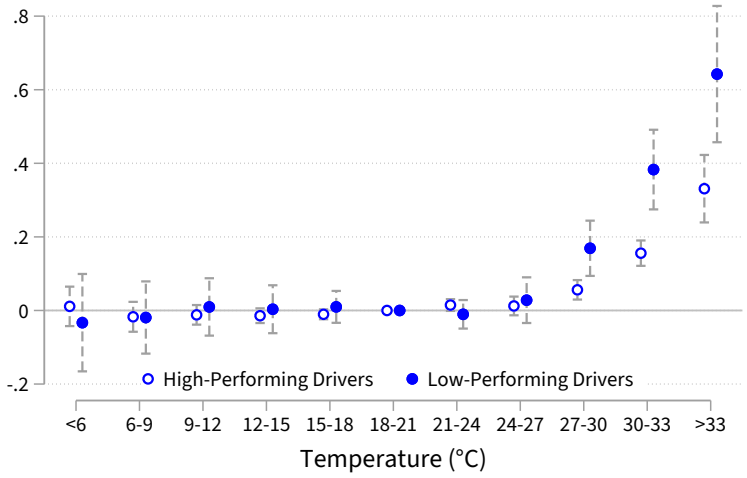


Figure 6: Effect of Heat on Adaptation: Resting Behaviors

Notes: This figure displays the estimated effects of hourly temperature exposure on the frequency and duration of rests. Short rests are defined as those lasting less than 1 hour, while long rests are those lasting more than 1 hour. The blue dots represent the point estimates, while the gray vertical caps indicate the corresponding 95% confidence intervals. Regression models include control variables such as other weather conditions, air quality, and geographic characteristics, along with vehicle fixed effects and date fixed effects. The temperature range of 18–21°C is the omitted category, serving as the reference group for comparison. Standard errors are clustered at the vehicle level.



(a) By Average Temperature Exposure



(b) By Driving Performance

Figure 7: Heterogeneity by Driving Experience

Notes: This figure displays the estimated effects of hourly temperature exposure on the number of alarms per 100 km of driving, separately by drivers' temperature exposure experience and driving performance. In Panel (a), drivers are classified into two groups based on whether their average temperature exposure is above (blue dots) or below 24°C (white dots). In Panel (b), drivers are categorized into two groups based on whether their average alarm intensity during days with mild temperatures (i.e., $\leq 24°$) is above (i.e., low-performing drivers) or below (i.e., high-performing drivers) the sample median, reflecting differences in driving performance. The dots represent the point estimates, while the gray vertical caps indicate the corresponding 95% confidence intervals. Each panel is a separately estimated regression model that includes control variables such as other weather conditions, air quality, and geographic characteristics, along with vehicle fixed effects and date fixed effects. The temperature range of 18–21°C is the omitted category, serving as the reference group for comparison. Standard errors are clustered at the vehicle level.

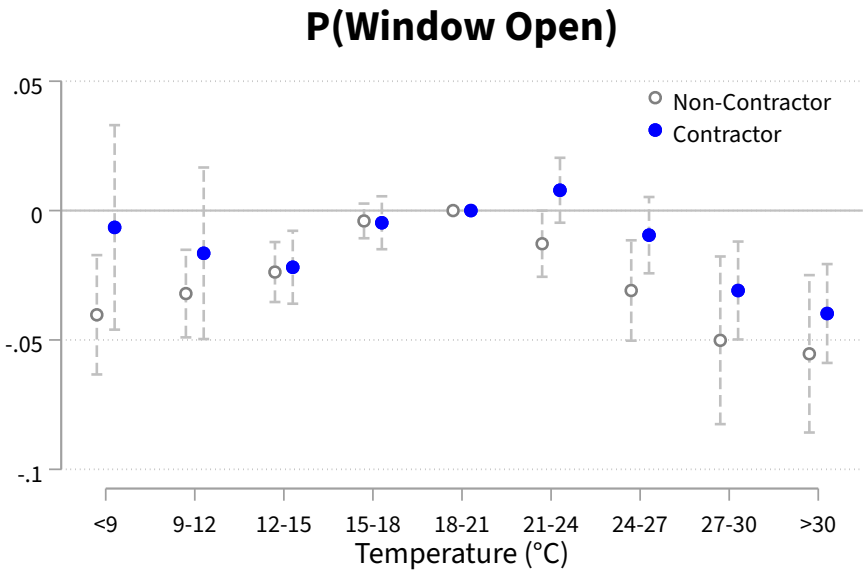


Figure 8: Heterogeneity Effects by Cost-Bearing Schemes: Probability of Driver-Side Window Being Open

Notes: This figure displays the estimated heterogeneous effects of temperature on the probability of driver-side window being open, separately by cost-bearing schemes. The analysis is based on a sample of in-cabin camera photos, with window status identified using computer vision techniques. The horizontal axis represents binary indicators for whether the contemporaneous temperature exposure falls within a specific range. The dots represent point estimates, while the gray vertical caps indicate corresponding 95% confidence intervals. The temperature range of 18–21°C is the omitted category, serving as the reference group for comparison. Regressions include other weather controls, driving speed, vehicle fixed effects, and fixed effects for year-by-month, day-of-week, hour-of-day. Standard errors are clustered at the vehicle level.

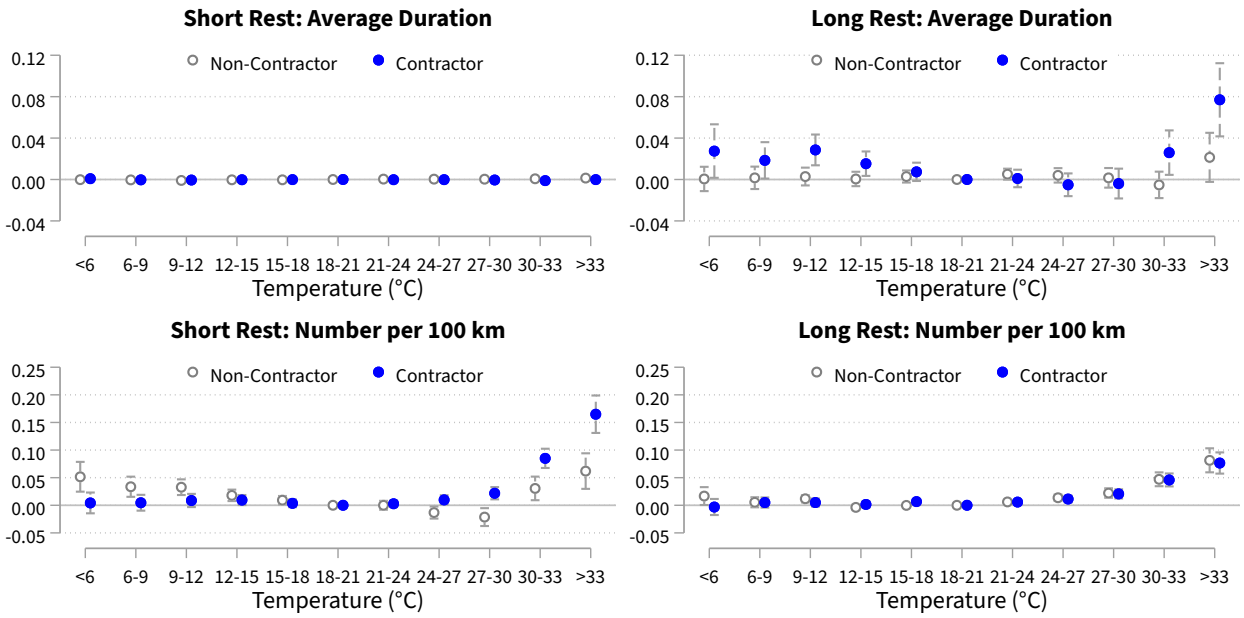
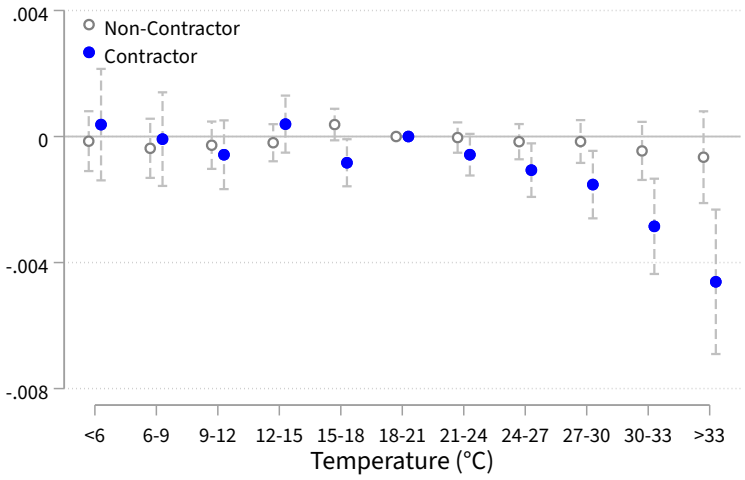
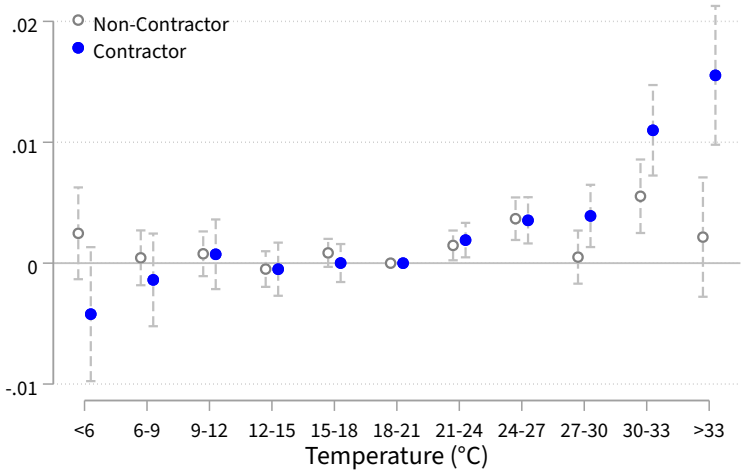


Figure 9: Effect of Heat on Resting Behavior by Cost-Bearing Schemes

Notes: This figure displays the estimated effects of hourly temperature exposure on resting behavior, separately by cost-bearing schemes. Short rests are defined as those lasting less than 1 hour, while long rests are those lasting more than 1 hour. For a subsample of vehicles whose company information is available, we classify them into two groups based on whether their companies operate as a contractor (blue dots) or not (white dots). The dots represent the point estimates, while the gray vertical caps indicate the corresponding 95% confidence intervals. Each panel is a separately estimated regression model that includes control variables such as other weather conditions, air quality, and geographic characteristics, along with vehicle fixed effects and date fixed effects. The temperature range of 18–21°C is the omitted category, serving as the reference group for comparison. Standard errors are clustered at the vehicle level.



(a) If driving on a day



(b) Starting work late than usual

Figure 10: Effect of Heat on Work Schedule Adjustment by Cost-Sharing Schemes

Notes: This figure displays the estimated effects of temperature on daily work schedule adjustment, separately by cost-sharing schemes. The outcome in Panel (a) is an indicator for whether a driver takes any driving task on a day. The outcome in Panel (b) is an indicator for whether a driver starts work later than their usual schedule. For a subsample of vehicles whose company information is available, we classify them into two groups based on whether their companies operate as a contractor (blue dots) or not (white dots). The dots represent the point estimates, while the gray vertical caps indicate the corresponding 95% confidence intervals. Each panel is a separately estimated regression model that includes control variables such as other weather conditions, air quality, and geographic characteristics, along with vehicle fixed effects and date fixed effects. The temperature range of 18–21°C is the omitted category, serving as the reference group for comparison. Standard errors are clustered at the vehicle level.

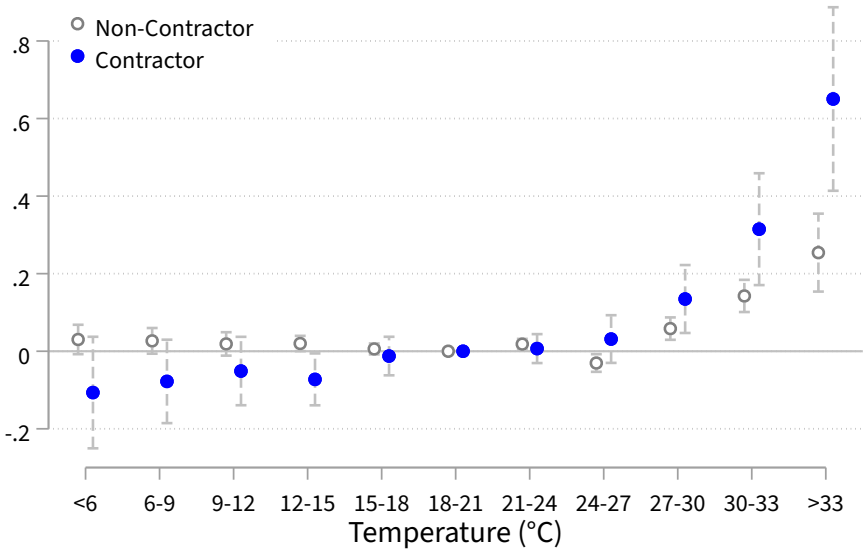


Figure 11: Heterogeneity by Cost-Bearing Schemes: Intensity of Dangerous Driving

Notes: This figure displays the estimated effects of hourly temperature exposure on the number of alarms per 100 km of driving, separately by cost-bearing schemes. For a subsample of vehicles whose company information is available, we classify them into two groups based on whether their companies operate as a contractor (blue dots) or not (white dots). The dots represent the point estimates, while the gray vertical caps indicate the corresponding 95% confidence intervals. Each panel is a separately estimated regression model that includes control variables such as other weather conditions, air quality, and geographic characteristics, along with vehicle-fixed effects and date fixed effects. The temperature range of 18–21°C is the omitted category, serving as the reference group for comparison. Standard errors are clustered at the vehicle level.

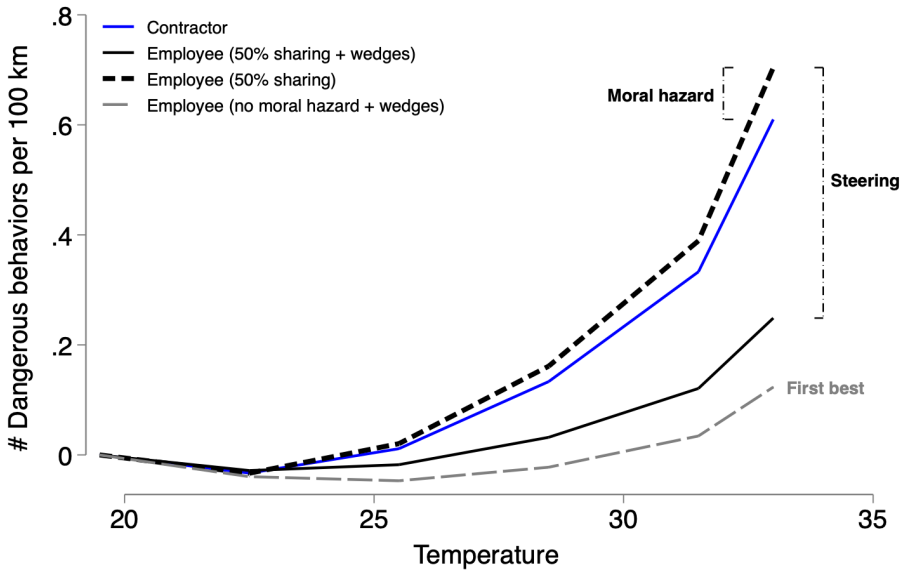


Figure 12: Counterfactual Decomposition of Employee-Contractor Differences

Notes: This figure decomposes the observed difference between employee and contractor drivers into a moral hazard component and a steering component. The moral hazard component compares contractors with employee drivers under cost-sharing but without firm steering. The steering component compares that counterfactual to the observed employee outcome under optimal firm steering.

7.1 Tables

Table 1: Summary Statistics

Variables	Mean	S.D.	Min.	Max.
Number of Alarms per 100km				
All	13.23	21.72	0.00	155.40
Outside Conditions				
Blind Spot	5.26	15.23	0.00	155.39
Lane Departure and Change	2.80	7.10	0.00	154.45
Following Too Closely	2.48	5.21	0.00	151.35
Collision	1.34	3.39	0.00	137.45
Speeding	0.01	0.67	0.00	93.92
Inside Conditions				
Driver Distracted	0.81	3.09	0.00	154.44
Fatigued Driving	0.31	1.39	0.00	152.83
Hands Off the Steering Wheel	0.00	0.12	0.00	42.53
Driving Distance and Speed				
Total Driving Distance in a Day (km)	151.26	112.53	0.25	557.68
Total Driving Hours in a Day	9.75	4.93	0.01	23.99
Mean Speed (km/h)	28.59	9.40	0.10	95.40
Rests				
Number of Long Rests per 100km	3.45	3.61	0.00	23.37
Number of Short Rests per 100km	5.18	4.83	0.00	28.04
Average Duration of Short Rests (h)	0.42	0.16	0.00	1.00
Average Duration of Long Rests (h)	4.59	3.05	0.00	24.00

Notes: This table reports summary statistics of key variables used in the analyses. Unit of observation is vehicle-day.

Table 2: Heterogeneous Effects of Heat by Alarm Category

VARIABLES	Outside Conditions					Inside Conditions		
	Blind Spot	Following Too Closely	Collision	Lane Departure	Speeding	Distraction	Fatigued	Hands off Steering Wheel
	(1)	(2)	(3)	(4)	(5)	(6)	(7)	(8)
>33°C	0.2023***	0.0781***	0.0401***	0.0285**	-0.0005**	0.0231***	0.0066**	0.0007***
	(0.0281)	(0.0097)	(0.0050)	(0.0143)	(0.0002)	(0.0072)	(0.0030)	(0.0003)
Outcome Mean	5.259	2.482	1.339	2.800	0.013	0.812	0.311	0.002
Observations	2,172,348	2,172,348	2,172,348	2,172,348	2,172,348	2,172,348	2,172,348	2,172,348

Notes: This table reports the estimated effects of temperature on the number of alarms per 100km of driving by alarm category. Each column is a separately estimated regression using Equation 1. We only report the coefficient estimates for the >33°C temperature category. Coefficient estimates for all temperature categories are presented in Figure D6. All regressions include control variables such as other weather conditions, air quality, and geographic characteristics, along with vehicle fixed effects and date fixed effects. The temperature range of 18–21°C is the omitted category, serving as the reference group for comparison. Standard errors are clustered at the vehicle level. * $p < 0.1$, ** $p < 0.05$, *** $p < 0.01$.

Table 3: Estimated Model Parameters

Variables	AC	Resting	Labor supply
Panel A. Adaptation behaviors			
γ_1^v	-0.030	-0.314	0.003
γ_2^v	0.091	0.184	0.132
γ_1^B	0.469	-0.215	-0.005
γ_2^B	-0.036	0.062	0.008
Panel B. Adaptation outcomes			
w	-0.250	0.000	-0.060
θ		0.5	

Notes: This table reports parameter estimates from the structural model. Panel A reports the parameters governing the temperature dependence of the private component v and the true marginal benefit B for each adaptation margin. Panel B reports the adaptation outcome weight w, which maps each adaptation margin into dangerous driving outcomes. The parameter θ governs the worker's share of benefits and costs under employee contracts.

Online Appendix

Steering Adaptation: Firm, Labor Contracts, and Driver Responses to Heat in the Trucking Industry

Wenzhi Dave Ding Xincheng Wang
Yucheng Wang Zhenxuan Wang

A Additional Details about Truck Monitoring System **SI-1**

B More Back-of-the-Envelope Results and Calculation Details **SI-2**

C Structure Model Estimation **SI-6**

D Additional Figures and Tables **SI-7**

A Additional Details about Truck Monitoring System

These services include installing sensors and cameras, using facial recognition technology to identify risky driving behaviors, immediate alerts to address potential dangers, and detailed reporting and analysis to monitor and improve driving practices. The risky driving alarm systems can be divided into three groups: Driver Monitoring Systems (DMS), Advanced Driver Assistance Systems (ADAS), and Blind Spot Detection (BSD). The Driver Monitoring System (DMS) is a camera-based system that uses an in-cabin camera to monitor the driver's face and eyes. It is designed to detect signs of fatigue or distraction, major contributors to road accidents. For instance, Figure 1 shows the driver used his phone while driving. By identifying when a driver may be too tired or inattentive, the DMS can issue warnings to prompt the driver to refocus or take a break. This system is crucial in promoting safe driving by reducing the risk of accidents caused by driver impairment or inattention.

The Advanced Driver Assistance System (ADAS) is a sensor-based system that enhances driving safety and reduces collision risks by using various sensors. The Lane Departure Warning (LDW) feature uses a camera to monitor lane markings and alerts drivers when they drift out of their lane without signaling, helping prevent accidents caused by distraction or fatigue. The Forward Collision Warning System (FCWS) employs radar or a camera to detect the distance and relative speed of the vehicle ahead, warning drivers of potential collision risks and prompting them to take evasive actions like slowing down or braking to avoid rear-end collisions. While the Driver Monitoring System (DMS) focuses on monitoring the internal state of the driver, ADAS concentrates on sensing and responding to the external environment surrounding the vehicle. The Blind Spot Detection (BSD) is a multi-approach-based system that monitors the areas around the vehicle that cannot be seen in the side mirrors, alerting the driver to other vehicles or objects in those blind spots. BSD systems commonly employ radar, cameras, or ultrasonic sensors to detect objects within the blind spot zones, and these sensors are typically mounted on the vehicle's side mirrors or within the radar system itself. Unlike DMS and ADAS, most warnings in BSD are driven by traffic conditions instead of drivers' behaviors.

B More Back-of-the-Envelope Results and Calculation Details

B1 Evaluating if Truck Drivers' Private Adaptation is Enough

To quantitatively compare the adaptation effort with the socially optimal level, we develop a simple model featuring negative externalities from heat exposure and drivers' choice of adaptation level with different cost-sharing arrangements.

Set-up. The driver i's utility depends on heat damage $D(t,a)$ and monetary cost of adaptation $A_i(a)$. $D(t,a)$ which is a function of heat exposure t and adaptation a. The driver's problem is,

$$\max_a U_i = -D(t,a) - A_i(a)$$

The first-order condition (FOC) is,

$$-D'_a(t,a) = A'_i(a) \tag{B1}$$

where D'_a is the partial derivative of $D(t,a)$ with respect to a. We assume that $D'_a < 0$, $D'_t > 0$, the temperature shocks damage driving performance and incur dangerous driving behaviors while adaptation costs alleviate it. To study how adaptation behavior responds to heat exposure, solving for $\frac{da}{dt}$:

$$\frac{da^*}{dt} = -\frac{D''_{at}}{D''_{aa} + A''_i(a)}.$$

We assume $D''_{at} < 0$, so that adaption behaviors reduce the marginal damage of temperature shocks. We also assume $D''_{aa} > 0$, namely, the marginal damage relief is decreasing *w.r.t* to adaptation efforts. D''_{aa} and $A''_i(a)$ are both > 0 so that the cost function is convex.

Socially Optimal Adaptation. The social planner (SP)'s problem is:

$$\max_{a_1,\dots,a_I} W = \sum_{i\in\mathcal{I}} \Big(-D(t,a_i) - A_i(a) \Big) - \underbrace{\sum_{i\in\mathcal{I}} \Big(C(a) - A_i(a) \Big)}_{\text{Cost widget}} - \underbrace{\Gamma\Big(D(t,a_1), \dots, D(t,a_I) \Big)}_{\text{Externality damage}}$$

Where $C(a)$ is the social cost of adaptation behaviors, e.g. the loss of productivity and revenue from resting or the additional diesel expense from turning on the A/C.[33] The

[33] We do not account for the additional environmental cost from added greenhouse gas emissions. Including it would change the magnitude of the cost-benefit analysis but would not change the optimal adaptation level

marginal externality damage is positive, $\Gamma'(\cdot) > 0$, which captures the idea that dangerous driving behaviors of truck drivers also harm other vehicles on the road by increasing the potential risk of collisions.

Heterogeneity in Cost-Sharing Scheme. Assume we have two types of drivers, with the first driver having higher marginal adaptation costs: $A'_{1,H}(a) > A'_{2,L}(a)$ for all a. We assume the first driver fully bears the social cost $A_{1,H}(a) = C(a)$. In our context, driver 1 can be regarded as the contractor, while driver 2 represents the non-contractor, with the truck fleet covering part of their adaptation costs.

Since $D''_{aa} > 0$, one can show that $a_1^* < a_2^*$. Since $D''_{at} < 0$, we have $D'_t(t, a_1^*) > D'_t(t, a_2^*)$. Therefore, lower marginal adaptation costs lead to more private adaptation efforts and less marginal damage from temperature shocks.

From Model to Empirics. In our empirical design, we provide direct evidence on the following key comparative statistics. First, Figure 2 shows that dangerous driving behavior increases with heat exposure, therefore $D'_t(t, a) > 0$. Second, Figure 6 confirms that adaptation behavior increases with heat exposure, $da^*/dt > 0$. Third, the heterogeneous effect between contractors and employees in Figure 11 confirms that the damage from heat is lower when private adaptation costs are lower, $D'_t(t, a_1^*) > D'_t(t, a_2^*)$.

Is Truck Drivers' Private Adaptation Enough? Now, we use the framework to compare the private adaptation effort with the socially optimal level. For simplicity, we assume no congestion effects; that is, the damage on driver i does not change the marginal damage from temperature shocks on driver j.[34] The FOC of SP's problem is then, for driver i,

$$-\Big(1 + \Gamma'\big(D(t, a_1)\big)\Big) \cdot D'_a(t, a) = \Big(C'(a) - A'_i(a)\Big) + A'_i(a) \tag{B2}$$

Comparing the Equation B2 with B1, we can see that the difference between SP and the driver's optimal behaviors comes from two components. The first component is marginal externality damage. It makes the left-hand side (LHS) of SP's FOC greater than the LHS of the driver's FOC because, from the social planner's perspective, the marginal benefit from adaptation behaviors is higher. The second component is the marginal adaptation cost widget. We assume that $C'(a) \geq A'_i(a)$ for all a, that is, the drivers bear most parts of the marginal adaptation cost. For the drive type 1, the right-hand side (RHS) of SP's and driver's FOC are the same. Therefore, the private adaptation efforts are insufficient compared to the socially optimal level, $a_1^* < a_1^{sp}$.

However, for the drive type 2, the right-hand side (RHS) of SP's FOC is greater than the driver's FOC. Since we have $A''_i(a) > 0$, $-D''_{aa} < 0$, and both the LHS and RHS

[34] There are no terms related to the interaction between D_i and D_j. In other words, we do not consider the "arms race" in this framework. For the model with the arms race, we refer readers to Li (2012); Anderson and Auffhammer (2014).

are greater than zero, the relative magnitude of private and socially optimal adaptation efforts for driver 2 is ambiguous. The intuition is that while the positive externality leads to insufficient private adaptation efforts, the partial private cost leads to potential over-adaptation behaviors. However, we can show that $a_2^* \leq a_2^{sp}$ *iff*,

$$A_2'(a) \geq C'(a)/\left(1+\Gamma'(D(t,a_2))\right) \tag{B3}$$

The RHS is social damage-adjusted marginal adaptation cost, where the (marginal) social cost is adjusted by the sum of (marginal) private damage and externality damage. Therefore, the private adaptation level is lower (higher) than the socially optimal level if the private marginal cost is greater (smaller) than the social damage-adjusted marginal adaptation cost.

To bring data to Equation B3, we calibrate two key statistics, $A'(a)/C'(a)$, namely, the share of marginal adaptation cost borne by truck drivers, and $\Gamma'(D(t,a_2))$, which represents the magnitude of the externality. For contractor, $A'(a)/C'(a)$ is one. For non-contractors, since the total adaptation cost is the sum of the cost of AC and the cost of resting, and the cost of AC is assumed to be shared by the company, we calibrate the share of the cost borne by the driver, $A'(a)/C'(a)$, as $\frac{Cost\ of\ Resting}{Cost\ of\ AC\ +\ Cost\ of\ Resting}$.[35]

The results are displayed in Panel A of Table D2. Based on our calculations, the cost of AC is approximately 6.25% of the total revenue, and the cost of resting (due to the loss of transportation capacity as measured by distance) under the condition of one additional hour of temperature exposure above 33°C is approximately 3.75% of the total revenue. Therefore, $A'(a)/C'(a) = 0.39$.[36] $\Gamma'(D(t,a_2))$ is calibrated using the data that for every truck occupant fatality, the average number of other road users killed is 4.88. Thus, $1/\left(1+\Gamma'(D(t,a_2))\right) = 0.17$ is smaller than 0.39. Therefore, both types of drivers' adaptation costs are lower than the socially optimal level.

B2 Parameters and Calculation Details.

Here, we list the formula used in the back-of-the-envelope calculation. Parameter values can be found in Table D4.

Change in crashes related to trucks = 2.42% * Total crashes related to trucks

M_1 = Monetary value from fatality, trucks = Total property loss from traffic crash * Share of crashes related to trucks.

M_2 = Monetary value from fatality, trucks = Total fatalities from traffic crash * Share of crashes related to trucks * VSL.

M_3 = Monetary value from fatality, trucks = Total fatalities from traffic crash * Share

[35] The parameters and calculation formula are elaborated in Table D5.

[36] This figure is similar to the survey results for the truck fleet, and it is roughly estimated that 45% of the total adaptation cost is not shared by the truck company.

of crashes related to trucks * 0.5 * (Value of injury, severe + Value of injury, minor).

Monetized effect of extreme temperature, total = 2.42% * (M_1 + M_2 + M_3).

Monetized effect of extreme temperature from externality = 2.42% * (M_1 * $\frac{\text{Factor of externality, fatality}}{\text{Factor of externality, fatality + 1}}$ + M_2 * $\frac{\text{Factor of externality, injury}}{\text{Factor of externality, injury + 1}}$).

Monetized effect of extreme temperature on truck driver = Monetized effect of extreme temperature, total - Monetized effect of extreme temperature from externality

C Structure Model Estimation

We estimate the model separately for the three main adaptation margins in the data: air conditioning, resting, and labor supply. For each margin $k \in \{\text{AC}, \text{rest}, \text{labor}\}$, let $Q_E^k(T)$ and $Q_C^k(T)$ denote the adaptation responses of employee and contractor drivers at temperature T, relative to a baseline temperature.

We parameterize

$$B^k \mid T \sim \mathcal{N}\left(\mu_B^k(T), 1\right), \tag{C1}$$

$$v^k \mid T \sim \mathcal{N}\left(\mu_v^k(T), 1\right), \tag{C2}$$

with

$$\mu_B^k(T) = \gamma_{1,B}^k T + \gamma_{2,B}^k T^2, \tag{C3}$$

$$\mu_v^k(T) = \gamma_{1,v}^k T + \gamma_{2,v}^k T^2. \tag{C4}$$

The direct adaptation cost c is normalized, and θ is calibrated from institutional information on cost-sharing.

Given a parameter vector

$$\Theta_k = \{\gamma_{1,B}^k, \gamma_{2,B}^k, \gamma_{1,v}^k, \gamma_{2,v}^k\},$$

we simulate model-implied adaptation responses for employees and contractors and estimate an auxiliary regression on both simulated and observed responses. We then choose Θ_k to minimize the distance between the simulated and empirical auxiliary coefficients using indirect inference:

$$\hat{\Theta}_k = \arg\min_{\Theta_k} \left(\hat{\phi}_k^{data} - \hat{\phi}_k^{sim}(\Theta_k)\right)' W \left(\hat{\phi}_k^{data} - \hat{\phi}_k^{sim}(\Theta_k)\right). \tag{C5}$$

In a second step, we map adaptation into outcomes. Let $Y_E(T)$ and $Y_C(T)$ denote performance outcomes, such as dangerous driving or productivity, for employee and contractor drivers. We assume that each adaptation margin k contributes to outcomes with weight w_k, so that

$$Y_E(T) = \sum_k w_k \cdot \mathbb{E}\left[\hat{B}_k \cdot \mathbf{1}\{\theta \hat{B}_k + \hat{v}_k - \tau_k^E(T) \geq c\} \mid T\right], \tag{C6}$$

$$Y_C(T) = \sum_k w_k \cdot \mathbb{E}\left[\hat{B}_k \cdot \mathbf{1}\{\hat{B}_k + \hat{v}_k \geq c\} \mid T\right]. \tag{C7}$$

The weights $\Psi = \{w_k\}_k$ are then estimated by matching model-implied outcome responses to their empirical counterparts.

D Additional Figures and Tables

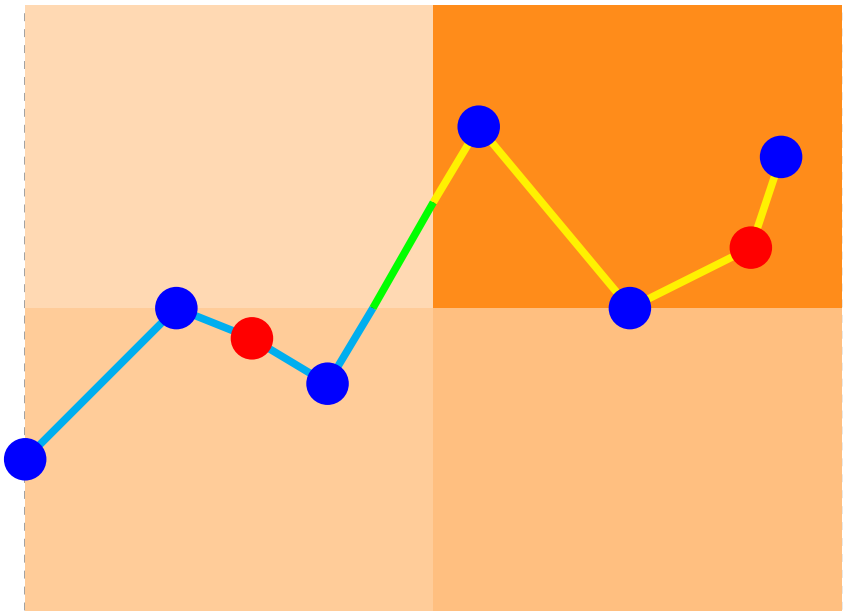


Figure D1: Illustration of Overlaying Truck-Route and Satellite Images

Notes: This figure illustrates how we spatially overlay the truck route data and rasterized data, e.g., temperature, and contribute to the heat exposure variables. All data are from the same hour, specifically 14:00–15:00, August 1, 2023, Beijing time. In the bottom layer, four rectangular stands for $0.1^\circ \times 0.1^\circ$ ($\approx$ 6.8 miles $\times$ 6.8 miles) pixels from the raw satellite image data. The blue dots represent the real-time GPS locations of the truck at 20-second intervals, while the red dots indicate warning recordings from the sensors. The truck's route is constructed by sequentially connecting both the red and blue dots based on their timestamps. The line segments overlaid between the route and the pixels are marked with different colors. Therefore, the length (and duration) of each colored line segment represents the continuous measurements of the truck's exposure in a temperature pixel.



(a) Yawning (Fatigued Driving)



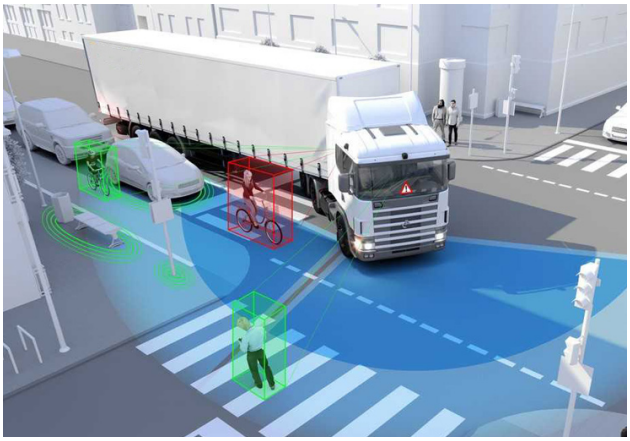
(b) Using Phone (Distracting)



(c) Smoking (Distracting)

Figure D2: Examples of Driver Monitoring System

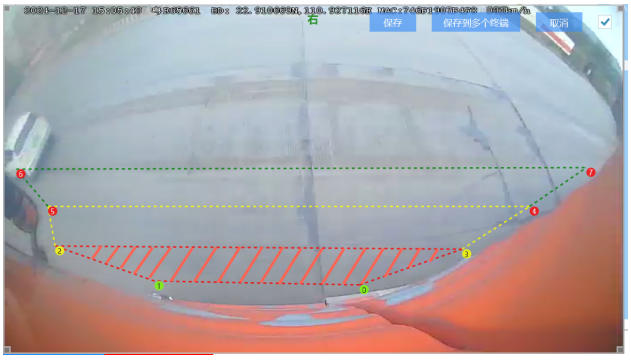
Notes: This figure shows camera snapshots of three examples where our Driver Monitoring Systems (DMS) detect dangerous driving behaviors. These behaviors are identified and classified using the face recognition algorithm. From top to bottom, these behaviors are yawning, using a cell phone, and smoking, which we classify as fatigued driving, distracting, and distracting, respectively.



(a) Example of Right Blind Spot



(b) Right Blind Spot Alarm Detection Zone, City



(c) Right Blind Spot Alarm Detection Zones, Highway

Figure D3: Illustration of Right Blind Spot Warning

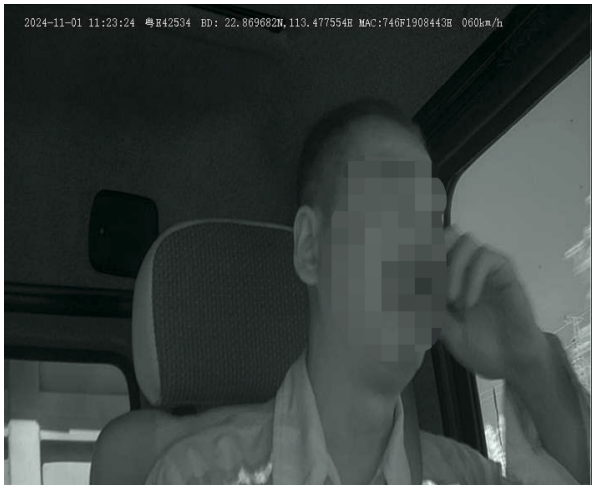
Notes: This figure illustrates the Blind Spot Detection (BSD) system.



(a) Example: Window is Opened



(b) Classify window is opened using computer vision algorithm



(c) Example: Window is Closed

Figure D4: Example of the Driver Opened the Window (A/C is off)

Notes: This figure displays camera snapshots where the cabin window was captured as being open. This observation suggests that, at that moment, the driver was most likely not using the AC system.

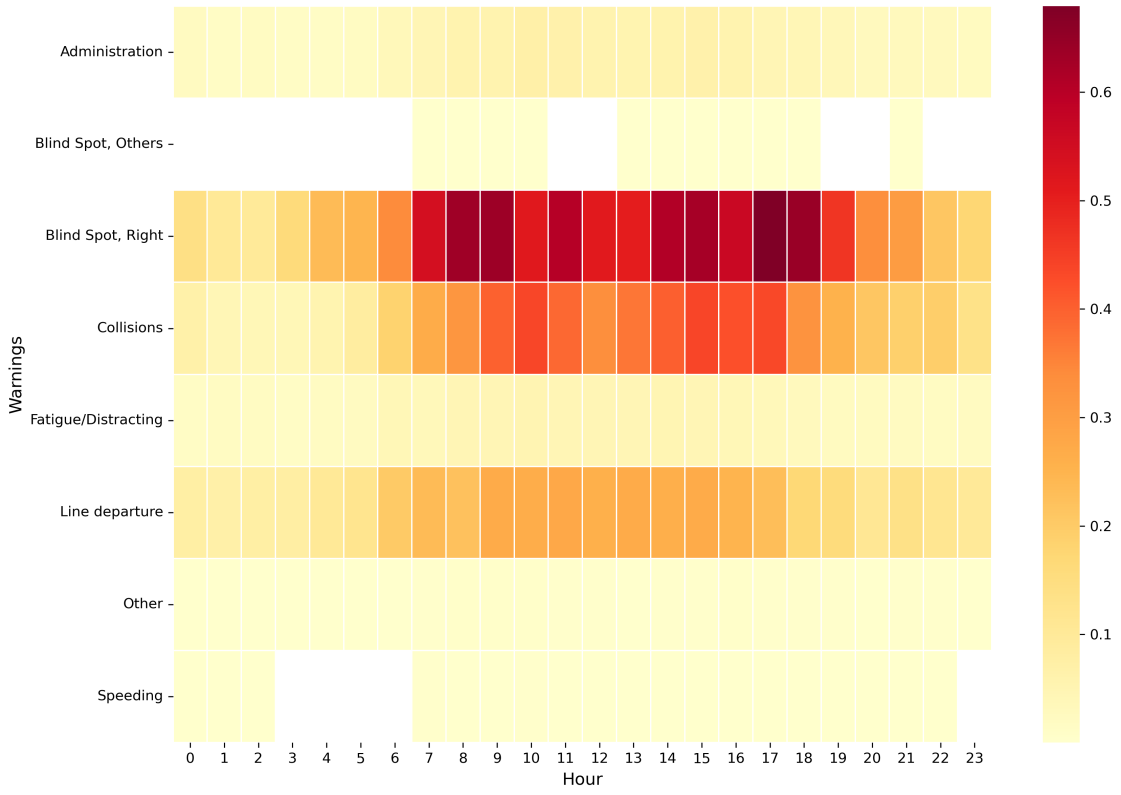


Figure D5: Average Number of Warning per Hour Over the Course of A Day

Notes: This figure shows the average number of each warning category per hour per truck in our sample from an example day, August 15, 2023. China is a left-hand drive country, meaning the driver and steering wheel are positioned on the left side of the vehicle. Therefore, the right blind spot is the major blind spot.

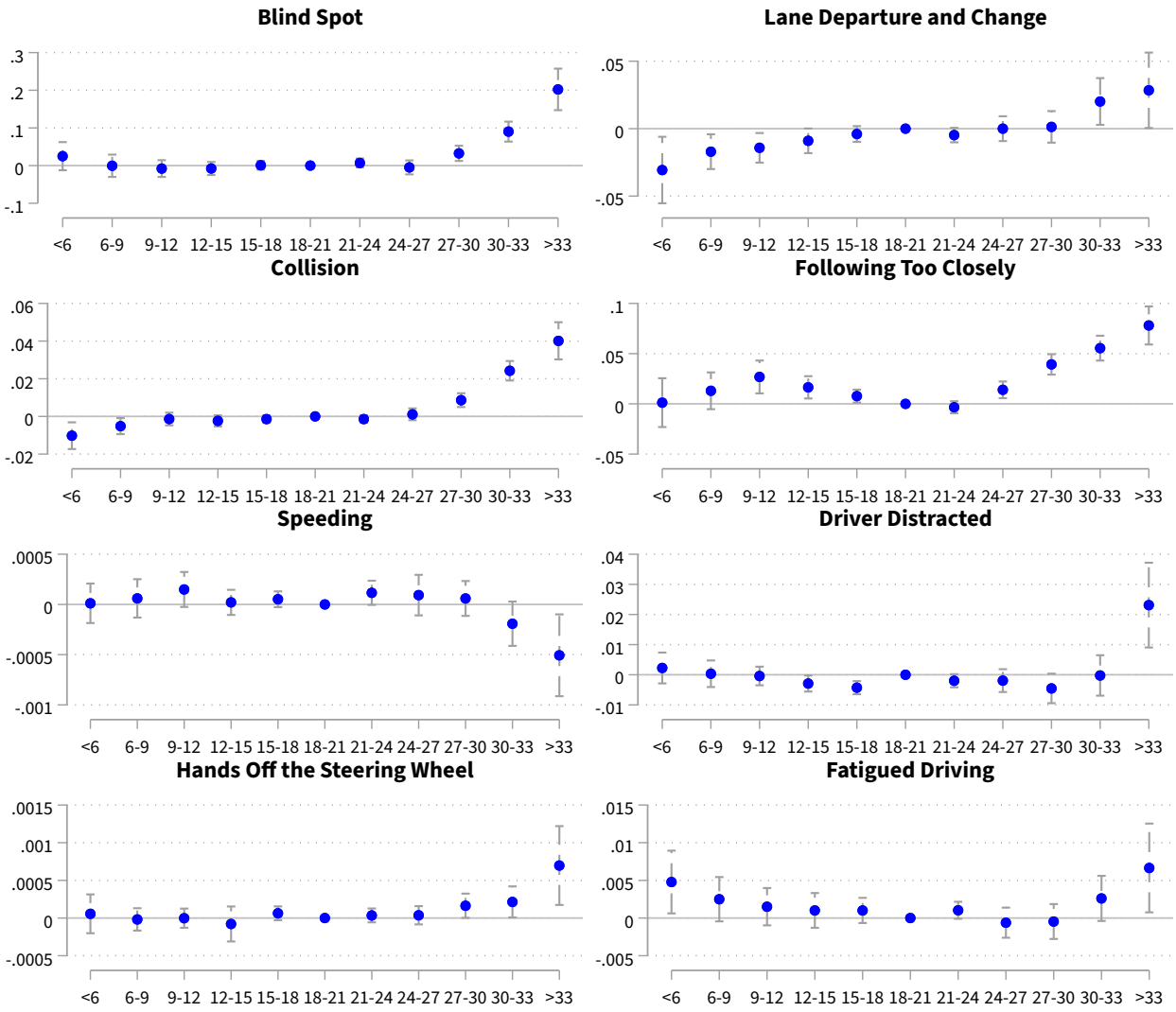


Figure D6: Heterogeneity by Alarm Category

Notes: This figure displays the estimated effects of hourly temperature exposure on the number of alarms per 100 km of driving, decomposed by alarm category. The blue dots represent the point estimates, while the gray vertical caps indicate the corresponding 95% confidence intervals. Each panel is a separately estimated regression model that includes control variables such as other weather conditions, air quality, and geographic characteristics, along with vehicle fixed effects and date fixed effects. The temperature range of 18–21°C is the omitted category, serving as the reference group for comparison. Standard errors are clustered at the vehicle level.

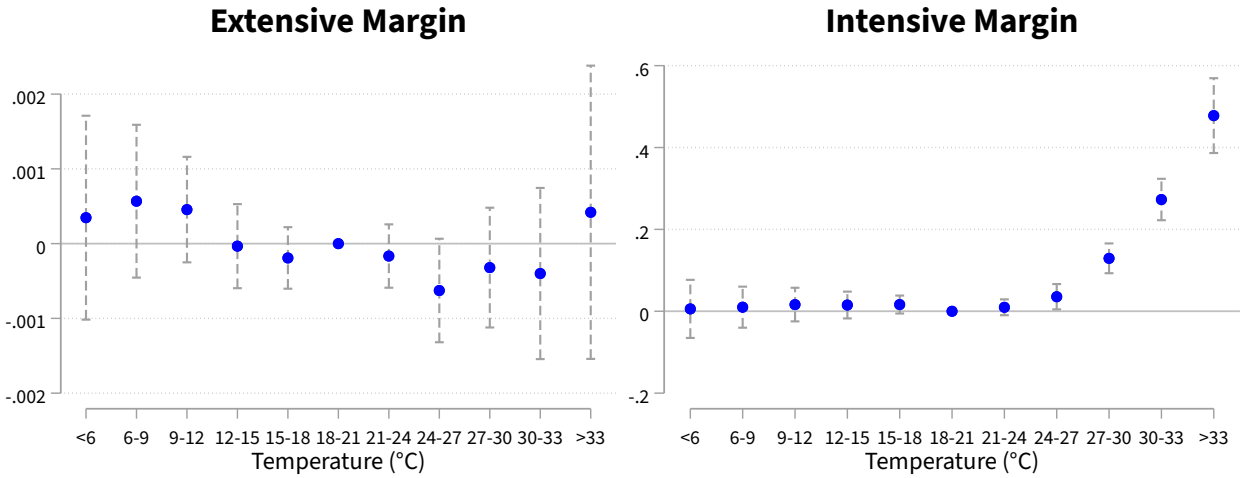


Figure D7: Effect of Heat - Intensive vs Extensive Margins

Notes: This figure presents the estimated effects of hourly temperature exposure on alarms, by the extensive and intensive margins. In the left panel, the outcome variable is a binary indicator for whether any alarm is triggered in a day, representing the extensive margin. In the right panel, the analysis is restricted to observations with positive alarm intensity, and the outcome variable is the number of alarms per 100 km of driving, capturing the intensive margin. The blue dots represent the point estimates, while the gray vertical caps indicate the corresponding 95% confidence intervals. The regression model includes control variables such as other weather conditions, air quality, and geographic characteristics, along with vehicle fixed effects and date fixed effects. The temperature range of 18–21°C is the omitted category, serving as the reference group for comparison. Standard errors are clustered at the vehicle level.

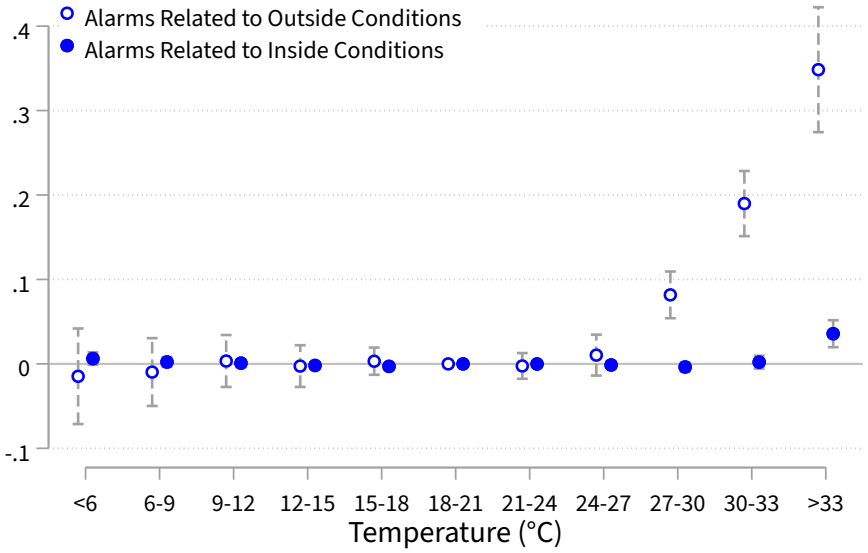
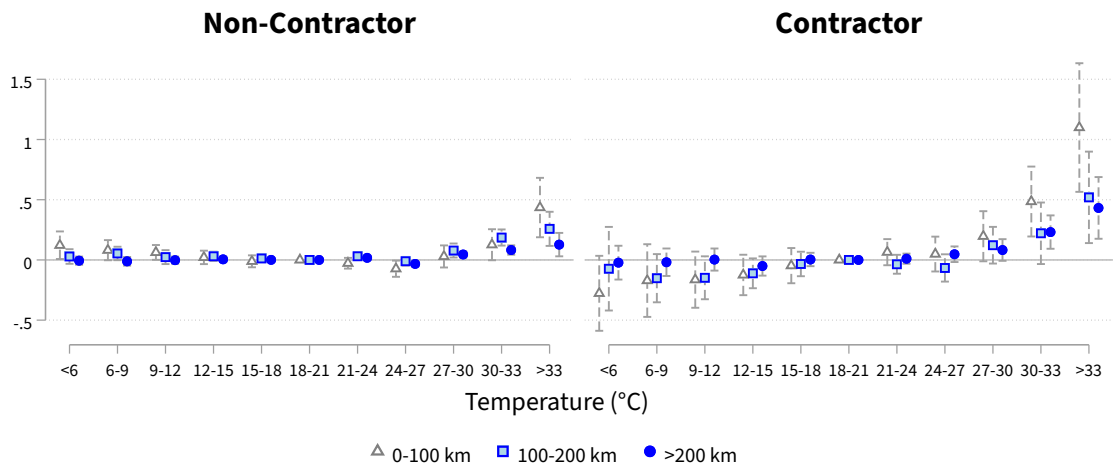
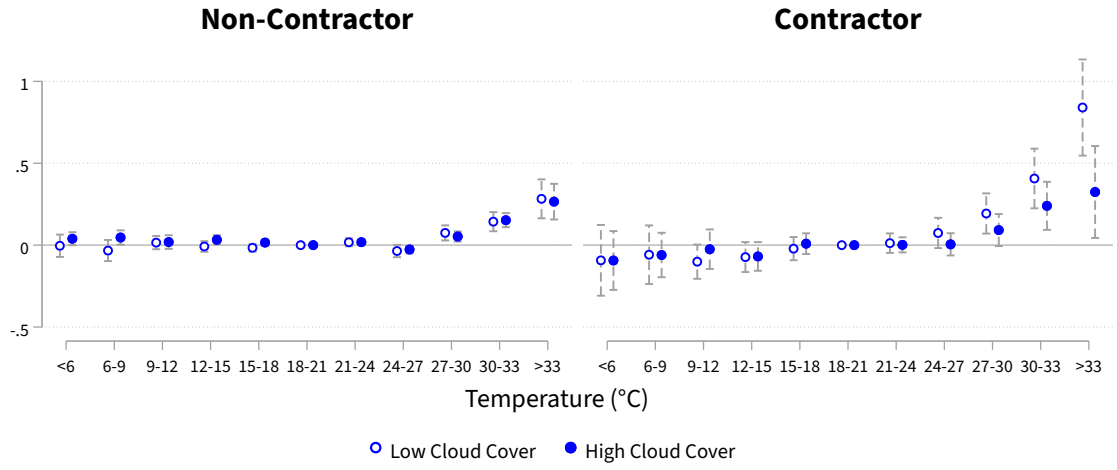


Figure D8: Heterogeneity by Alarms Related to Inside vs Outside Conditions

Notes: This figure displays the estimated effects of hourly temperature exposure on the number of alarms per 100 km of driving separately for alarms related to outside and inside conditions. The classification of alarms into these two categories is detailed in Table 1. The blue dots represent the point estimates, while the gray vertical caps indicate the corresponding 95% confidence intervals. Regression models include control variables such as other weather conditions, air quality, and geographic characteristics, along with vehicle-fixed effects and date-fixed effects. The temperature range of 18–21°C is the omitted category, serving as the reference group for comparison. Standard errors are clustered at the vehicle level.



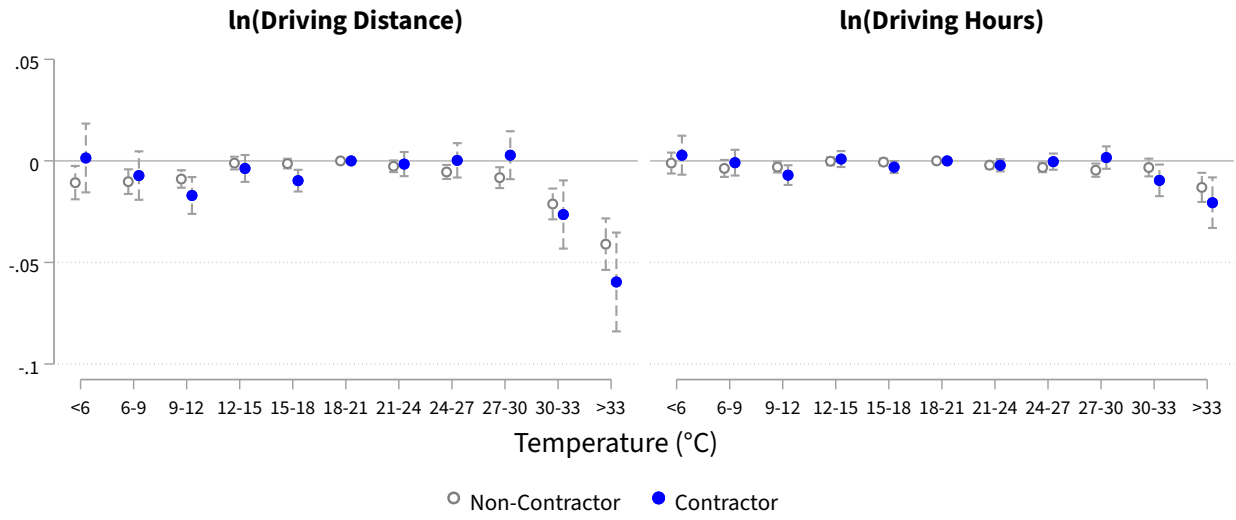
(a) By Driving Distance



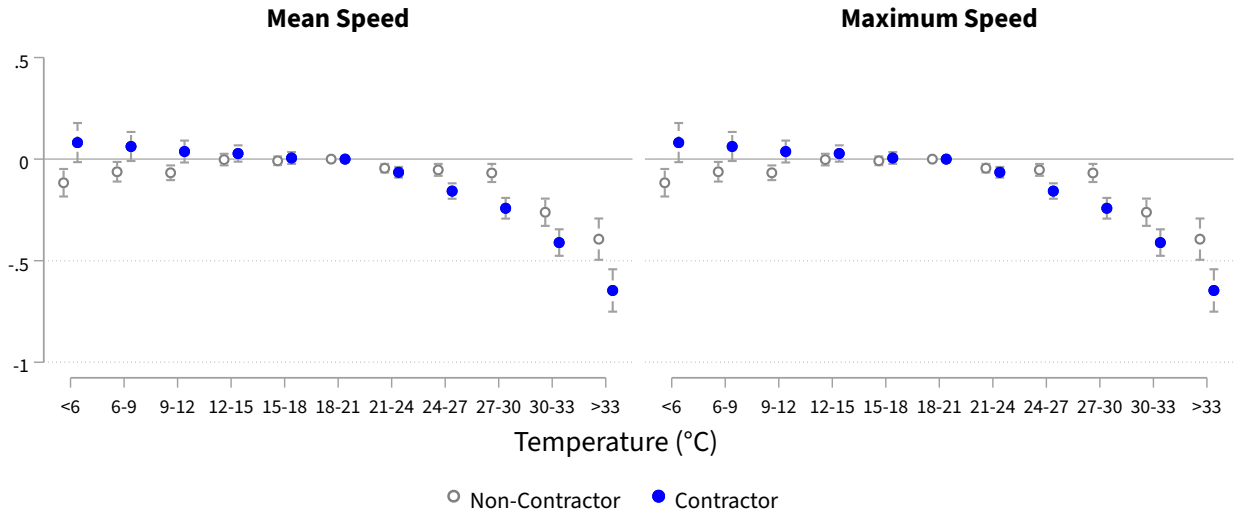
(b) By Cloud Cover

Figure D9: Heterogeneity by Cost-Bearing Schemes - Driving Distance & Cloud Cover

Notes: This figure displays the estimated heterogeneous effects of hourly temperature exposure on the number of alarms per 100 kilometers of driving, separately by cost-bearing schemes, driving distance, and cloud conditions. For a subsample of vehicles whose company information is available, we classify them into two groups based on whether their companies operate as a contractor or not. Panel (a) presents the estimated effects separately by driving distance. We further classify our sample into three groups based on the total driving distance in a day: below 100km, 100-200km, and above 200km, and estimate the effect separately for each group. Panel (b) presents the estimated effects separately by cloud cover conditions. Cloud cover, defined as the proportion of the area covered by clouds, is measured using ERA5 data. We classify the sample into two groups based on whether the average share of cloud cover is above (blue dots) or below (white dots) the median. The dots represent the point estimates, while the gray vertical caps indicate the corresponding 95% confidence intervals. Each panel is a separately estimated regression model that includes control variables such as other weather conditions, air quality, and geographic characteristics, along with vehicle fixed effects and date fixed effects. The temperature range of 18–21°C is the omitted category, serving as the reference group for comparison. Standard errors are clustered at the vehicle level.



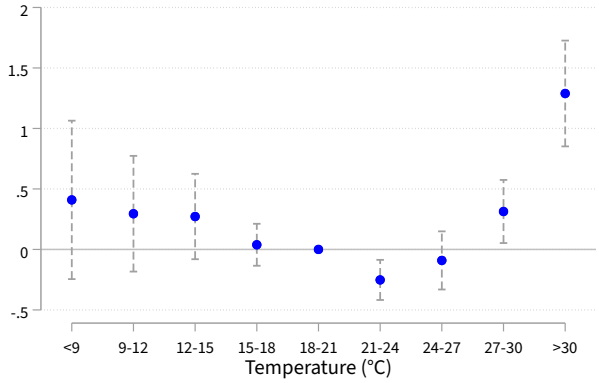
(a) Driving Distance and Hours



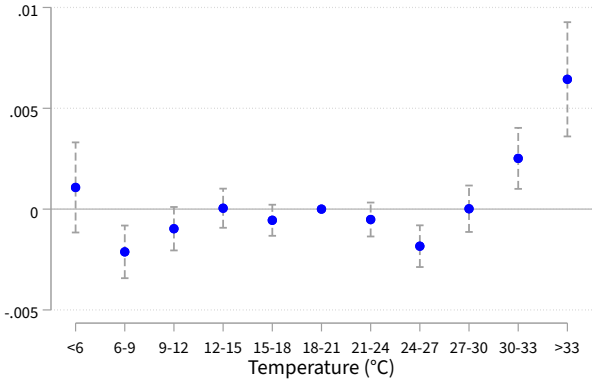
(b) Driving Speed

Figure D10: Effect of Heat on Driving Intensity and Speed by Cost-Bearing Schemes

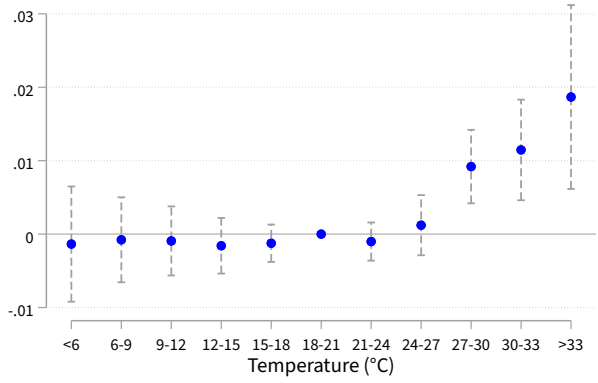
Notes: This figure displays the estimated effects of hourly temperature exposure on driving activities, separately by cost-bearing schemes. Panel (a) presents logarithm of driving distance (km) and hours. Panel (b) presents mean and maximum speed (km/h). For a subsample of vehicles whose company information is available, we classify them into two groups based on whether their companies operate as a contractor (blue dots) or not (white dots). The dots represent the point estimates, while the gray vertical caps indicate the corresponding 95% confidence intervals. Each panel is a separately estimated regression model that includes control variables such as other weather conditions, air quality, and geographic characteristics, along with vehicle fixed effects and date fixed effects. The temperature range of 18–21°C is the omitted category, serving as the reference group for comparison. Standard errors are clustered at the vehicle level.



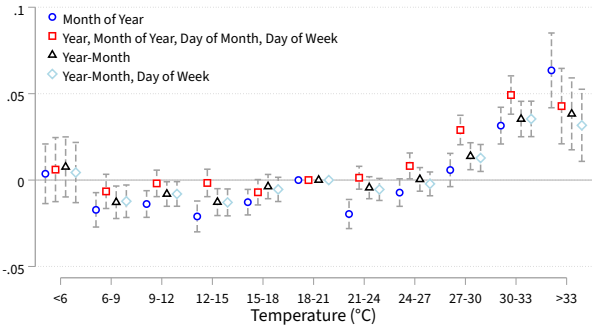
(a) Dummies of Daily Temperature Exposure



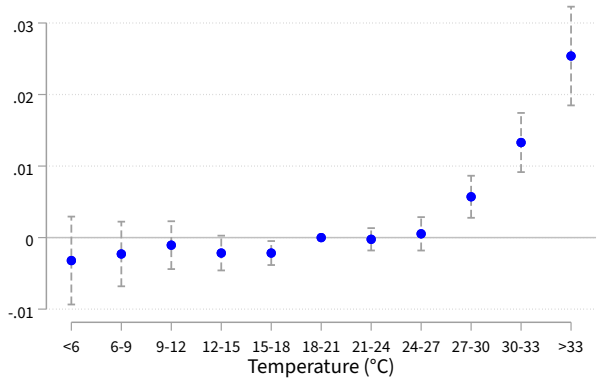
(b) Temperature Exposure by Driving Distance



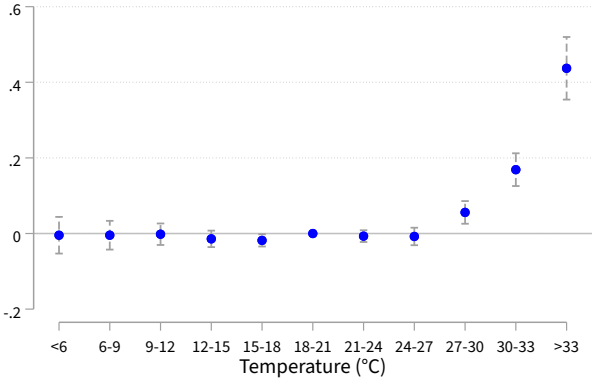
(c) Total Alarms Per Driving Hour



(d) Alternative Time Fixed Effects



(e) Poisson Regression



(f) Unweighted Regression

Figure D11: Robustness Checks - Alternative Model Specifications

Notes: This figure displays the estimated effects (point estimates and 95% confidence intervals) using alternative model specifications. Panel (a) uses indicators for whether the daily average temperature exposure falls within specific ranges. Panel (b) uses the driving distance exposed to each temperature range. Panel (c) estimates the effects on the number of alarms per driving hour. Panel (d) estimates the model using alternative time fixed effects. Panel (e) estimates a Poisson regression model. Panel (f) uses unweighted regression. The temperature range of 18–21°C is the omitted category, serving as the reference group for comparison. Standard errors are clustered at the vehicle level.

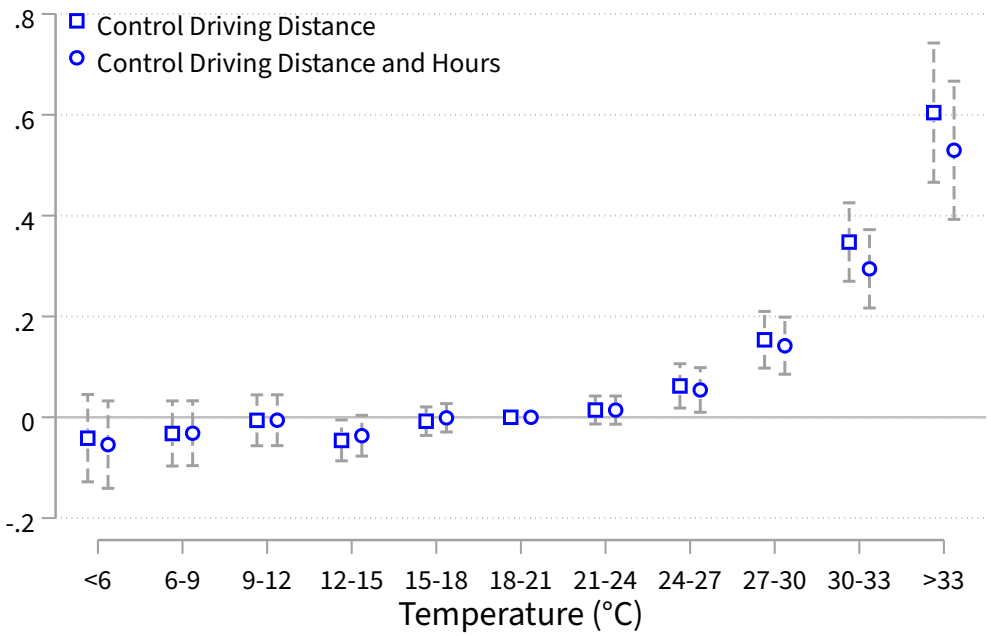


Figure D12: Robustness Checks - Using Total Number of Alarms

Notes: This figure displays the estimated effects (point estimates and 95% confidence intervals) of hourly temperature exposure on the total number of alarms, using two alternative model specifications: one controlling for daily driving distance and the other controlling for both daily driving distance and driving hours. All regression models include control variables such as other weather conditions, air quality, and geographic characteristics, along with vehicle fixed effects and date fixed effects. The temperature range of 18–21°C is the omitted category, serving as the reference group for comparison. Standard errors are clustered at the vehicle level.

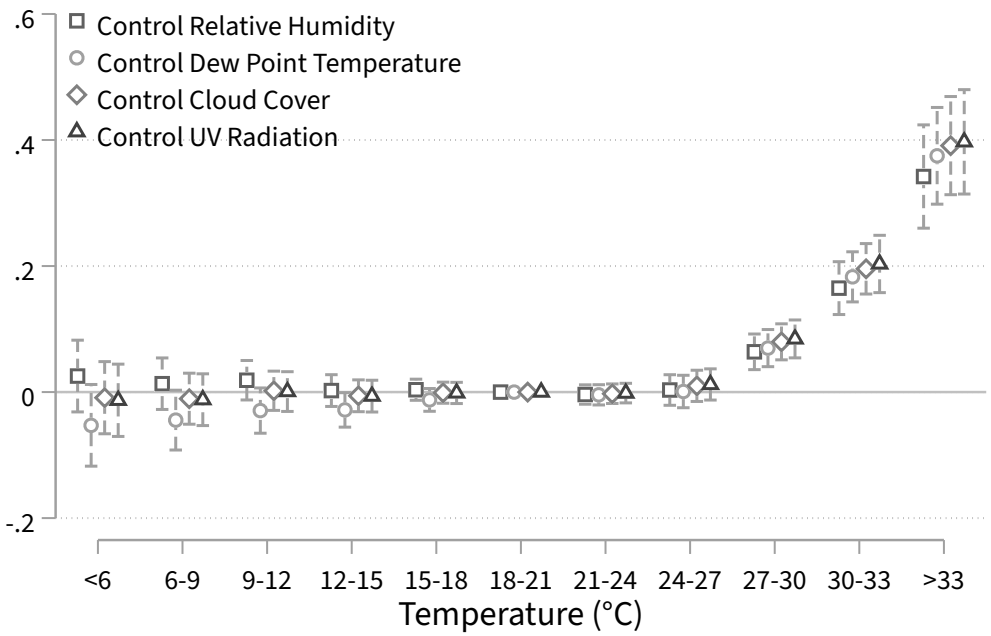


Figure D13: Robustness Checks - Control Other Weather Conditions

Notes: This figure displays the estimated effects (point estimates and 95% confidence intervals) of hourly temperature exposure on the total number of alarms per 100 kilometers of driving, controlling for additional meteorological conditions. The regression model includes control variables such as other weather conditions, air quality, and geographic characteristics, along with vehicle fixed effects and date fixed effects. The temperature range of 18–21°C is the omitted category, serving as the reference group for comparison. Standard errors are clustered at the vehicle level.

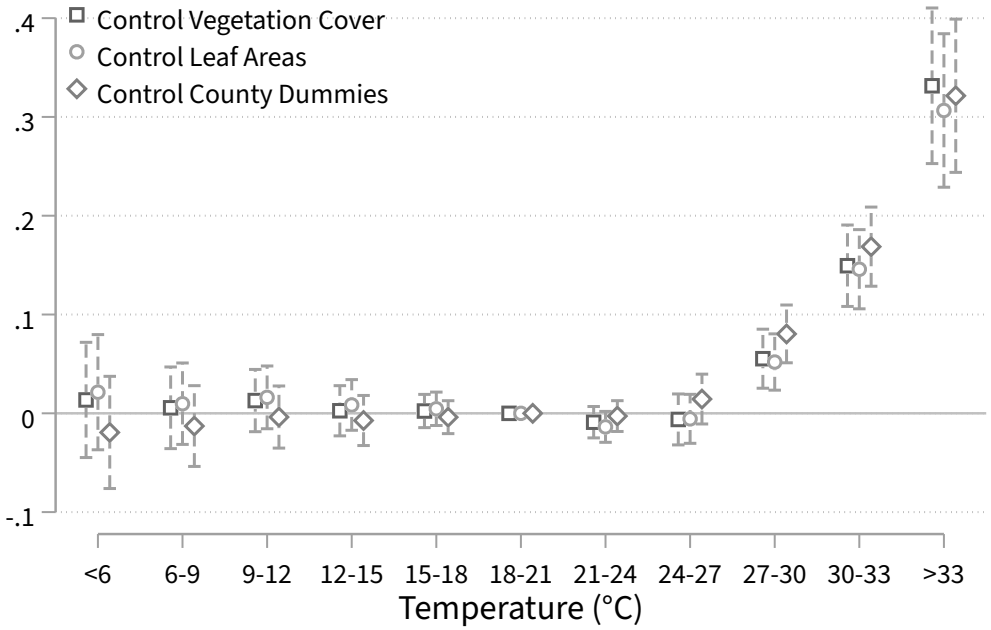
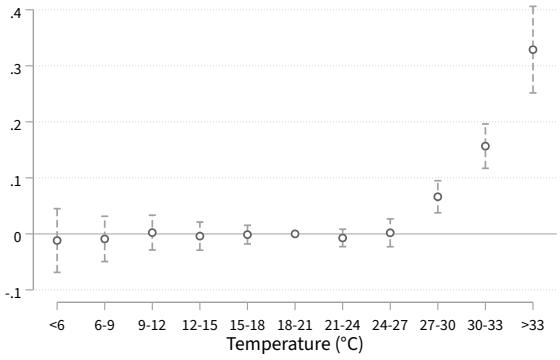
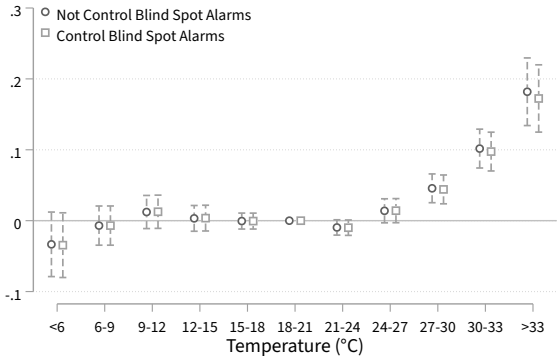


Figure D14: Robustness Checks - Control Other Road Conditions

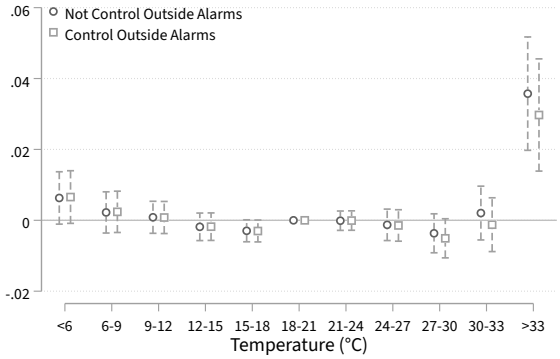
Notes: This figure displays the estimated effects (point estimates and 95% confidence intervals) of hourly temperature exposure on the total number of alarms per 100 kilometers of driving, controlling for additional road conditions. The regression model includes control variables such as other weather conditions, air quality, and geographic characteristics, along with vehicle fixed effects and date fixed effects. The temperature range of 18–21°C is the omitted category, serving as the reference group for comparison. Standard errors are clustered at the vehicle level.



(a) Control Mean Speed



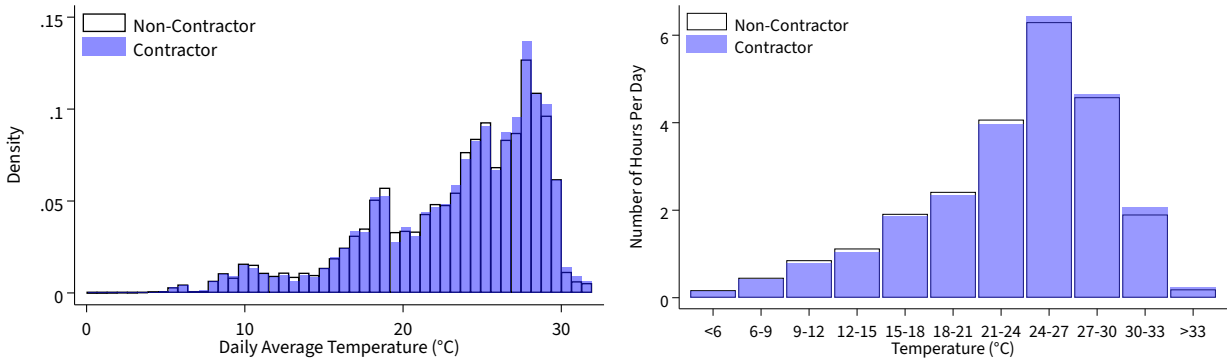
(b) Control Blind Spot Alarms



(c) Control Alarms Related to Outside Conditions

Figure D15: Robustness Checks - Traffic Conditions

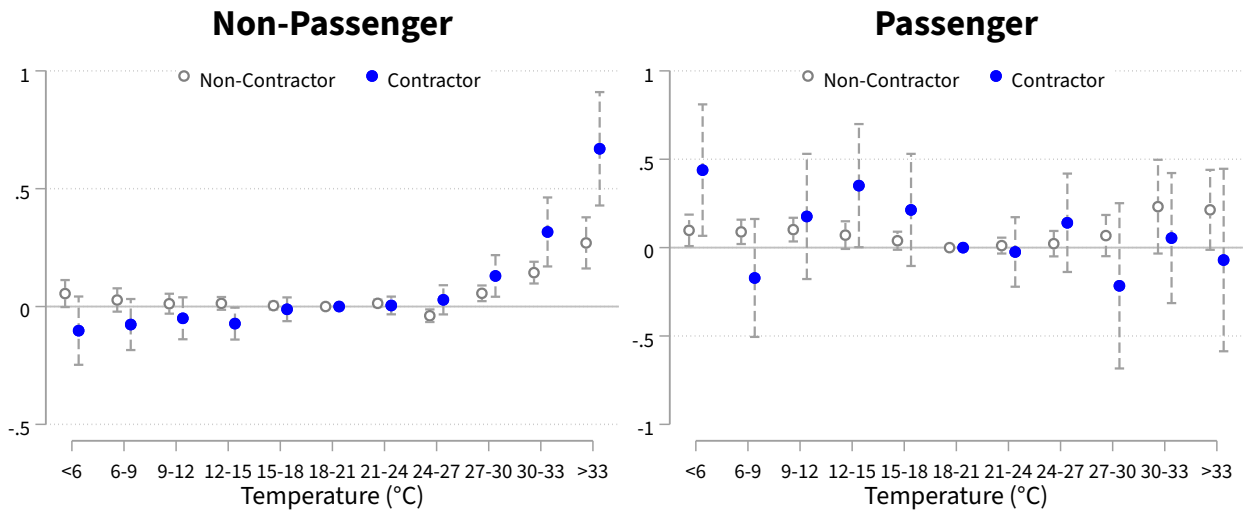
Notes: This figure displays the estimated effects (point estimates and 95% confidence intervals) of hourly temperature exposure on the total number of alarms per 100 km of driving, controlling for different measures of traffic conditions. Panel (a) includes mean speed as a control variable. In Panel (b), we estimate the effect of temperature on the number of alarms unrelated to blind spots per 100 km, with and without controlling for the number of blind spot alarms per 100 km. In Panel (c), we estimate the effect of temperature on the number of alarms related to inside conditions per 100 km, with and without controlling for the number of alarms related to outside conditions per 100 km. The regression model includes control variables such as other weather conditions, air quality, and geographic characteristics, along with vehicle fixed effects and date fixed effects. The temperature range of 18–21°C is the omitted category, serving as the reference group for comparison. Standard errors are clustered at the vehicle level.



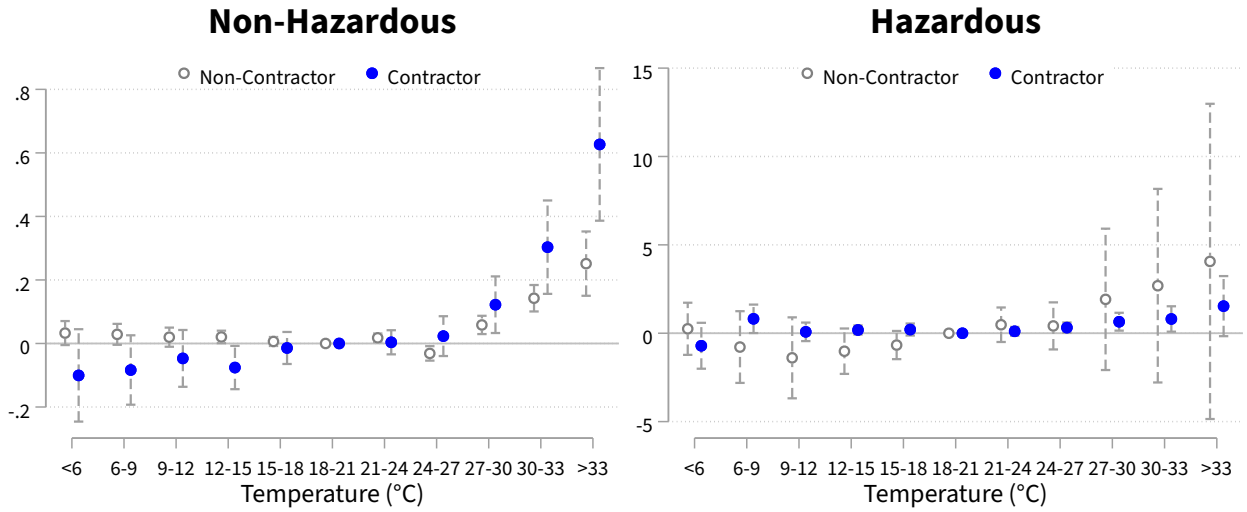
(a) Histogram of Daily Average Temperature (b) Distribution of Hourly Temperature within a Day

Figure D16: Temperature Distribution - Contractor vs Non-Contractor

Notes: This figure plots the distribution of temperature exposure by contractor vs non-contractors. Panel (a) shows the histogram of daily average temperature exposure. Panel (b) shows the average number of hours per day that drivers are exposed to temperatures within specific ranges.



(a) Passenger vs Non-Passenger Transportation



(b) Hazardous vs Non-Hazardous Cargo

Figure D17: Heterogeneity by Cost-Bearing Schemes - Transport Category

Notes: This figure displays the estimated heterogeneous effects of hourly temperature exposure on the number of alarms per 100 kilometers of driving, separately by cost-bearing schemes and transportation category. For a subsample of vehicles whose company information is available, we classify them into two groups based on whether their companies operate as a contractor or not. Panel (a) presents the estimated effects separately by passenger vs non-passenger transportation. Panel (b) presents the estimated effects separately for the transportation of hazardous cargo vs non-hazardous cargo. The dots represent the point estimates, while the gray vertical caps indicate the corresponding 95% confidence intervals. Each panel is a separately estimated regression model that includes control variables such as other weather conditions, air quality, and geographic characteristics, along with vehicle fixed effects and date fixed effects. The temperature range of 18–21°C is the omitted category, serving as the reference group for comparison. Standard errors are clustered at the vehicle level.

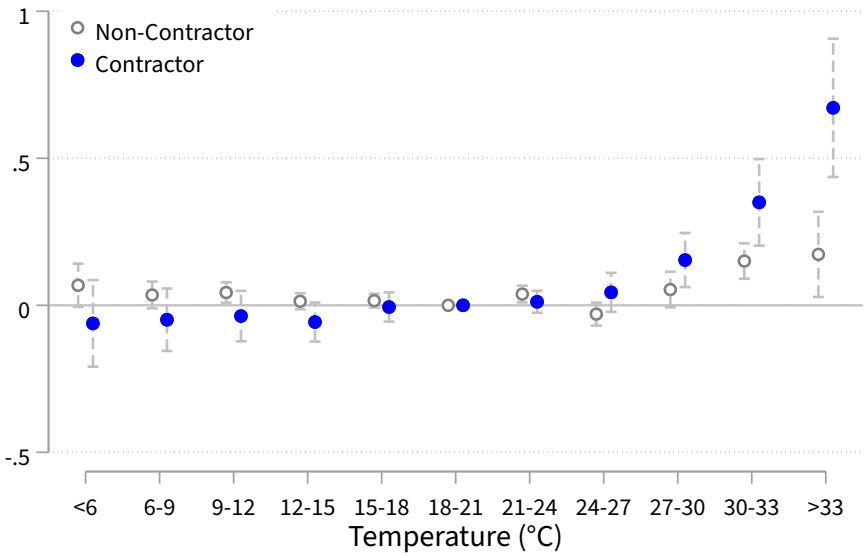
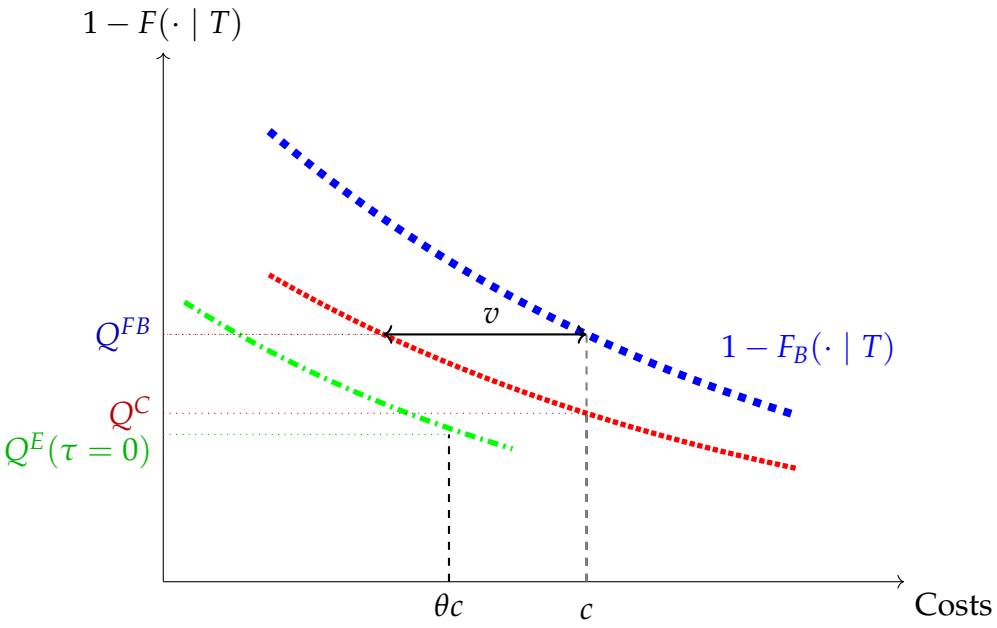
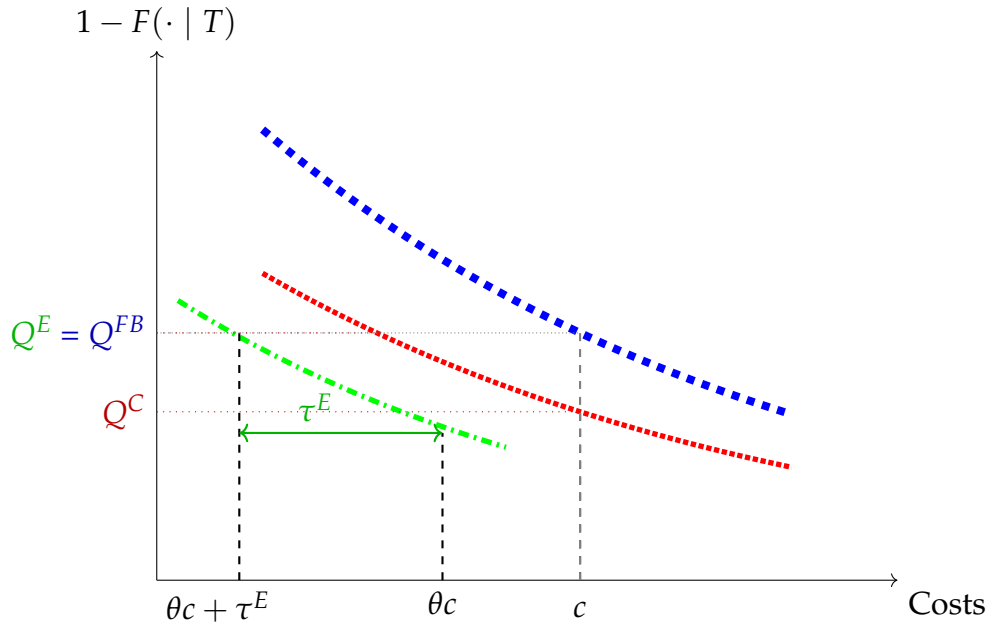


Figure D18: Heterogeneity by Cost-Bearing Schemes – Control Baseline Performance

Notes: This figure displays the estimated heterogeneous effects of hourly temperature exposure on the number of alarms per 100 kilometers of driving, separately by cost-bearing schemes. For a subsample of vehicles whose company information is available, we classify them into two groups based on whether their companies operate as a contractor or not. The dots represent the point estimates, while the gray vertical caps indicate the corresponding 95% confidence intervals. The regression models include control variables such as other weather conditions, air quality, and geographic characteristics, along with vehicle fixed effects and date fixed effects. The regression models include control variables for other weather conditions, air quality, and geographic characteristics, as well as vehicle fixed effects and date fixed effects. To account for drivers' baseline performance, we calculate each driver's average alarm intensity, average speed, and number of short rests per 100 km of driving on days with mild temperatures (i.e., $\leq$24°C). We then include interaction terms between the duration of temperature exposure in each bin and the demeaned baseline performance measures to flexibly control for heterogeneous temperature responses attributed to drivers' typical performance. The temperature range of 18–21°C is the omitted category, serving as the reference group for comparison. Standard errors are clustered at the vehicle level.



(a) Under-adaptation without firm steering



(b) Firm steering through τ^E

Figure D19: Illustration of the model mechanism

Notes: Panel A illustrates the case with $\theta < 1$, $\mathbb{E}[B] = c$, and $\mathbb{E}[v] < 0$. In the absence of firm steering, employee drivers adapt less than contractors because they internalize only a fraction of the true return to adaptation. Both groups under-adapt relative to the first best, but the gap is larger for employees. Panel B shows how the firm uses the wedge τ^E to shift employee behavior toward the firm's preferred adaptation level. When the average private wedge is negative, the optimal τ^E is negative and effectively lowers the cost of adaptation for employee drivers.

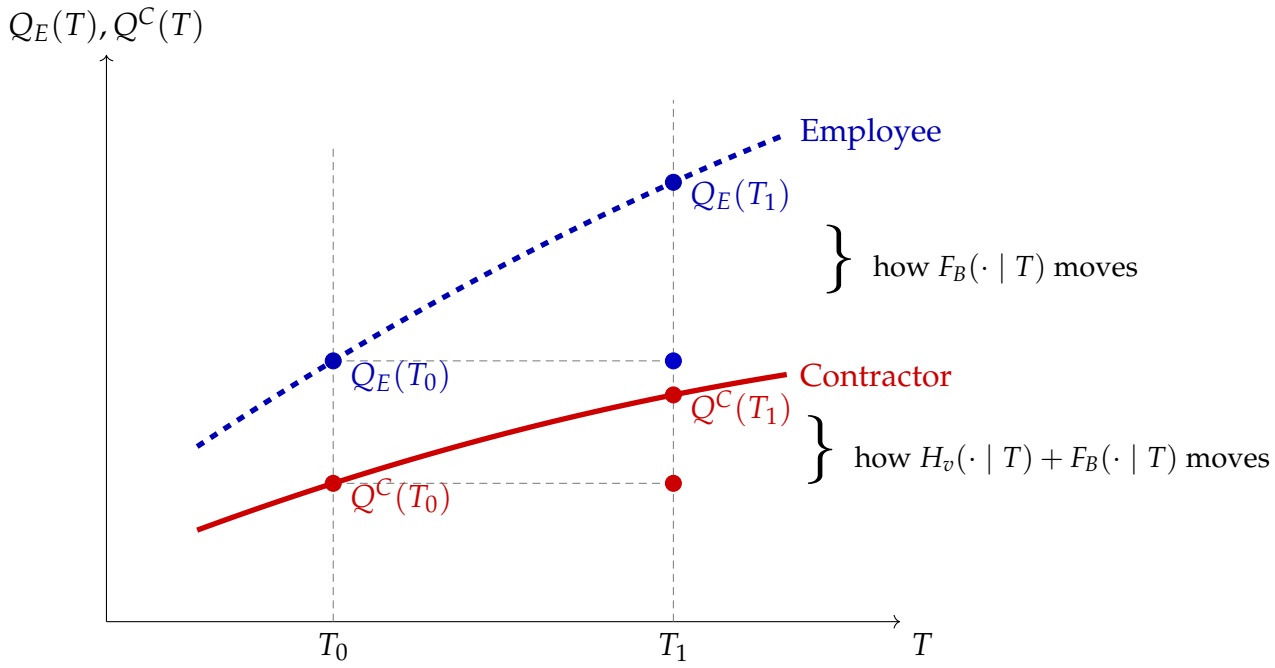


Figure D20: Identification through Temperature Shocks

Notes: As temperature rises from T_0 to T_1, the employee response identifies how the distribution of true marginal benefits, $F_B(\cdot \mid T)$, shifts with temperature. The contractor response reflects both the change in $F_B(\cdot \mid T)$ and the change in the private component, $H_v(\cdot \mid T)$. The gap between the two therefore identifies how the private wedge evolves with temperature.

Table D1: Balance Check - Contractor vs Non-Contractor

	(1) Non-Contractor	(2) Contractor	(3) Difference
Number of Alarms per 100km	12.564	15.554	2.990
	(8.745)	(8.380)	(2.202)
Total Driving Hours in a Day	8.721	8.724	0.003
	(3.445)	(1.240)	(0.762)
Total Driving Distance in a Day (km)	133.639	155.398	21.759*
	(53.226)	(45.343)	(13.025)
Mean Speed (km/h)	29.401	29.799	0.398
	(6.273)	(5.019)	(1.515)
Number of Short Rests per 100km	3.288	3.277	-0.011
	(1.272)	(1.286)	(0.325)
Number of Long Rests per 100km	4.722	4.563	-0.159
	(3.024)	(2.456)	(0.733)
Average Duration of Short Rests (h)	0.417	0.417	-0.000
	(0.037)	(0.028)	(0.009)
Average Duration of Long Rests (h)	4.753	5.005	0.252
	(1.358)	(0.892)	(0.317)
Passenger Transportation	0.286	0.018	-0.268**
	(0.463)	(0.135)	(0.102)
Hazardous Cargo	0.095	0.055	-0.041
	(0.301)	(0.229)	(0.072)
Average Temperature (°C)	23.230	23.453	0.223
	(1.344)	(0.892)	(0.314)
Wind Speed (m/s)	2.346	2.391	0.045
	(0.475)	(0.245)	(0.108)
Precipitation (m)	0.004	0.004	-0.000
	(0.001)	(0.000)	(0.000)
Air Quality Index	39.488	39.236	-0.252
	(1.995)	(1.522)	(0.477)
Number of Companies	21	55	

Notes: This table reports summary statistics for key variables, separated by whether companies operate as contractors or non-contractors. Columns (1) and (2) report the mean and standard deviation (in parentheses) for each group. Column (3) displays the difference in means between the two groups, along with the corresponding robust standard errors (in parentheses). * $p < 0.1$, ** $p < 0.05$, *** $p < 0.01$.

Table D2: Optimal Adaptation Level and Back-of-the-Envelope Calculations

Type	Statistics	Values
Panel A. Comparison Private and Social-Optimal Adaptation $a^* \leq a^{sp}$ *iff* Equation B3 holds		
Contractor	$A'(a)/C'(a)$	1
Contractor	$\Gamma'(D(t,a))$	4.88[a]
Contractor	$a^* \leq a^{sp}$	Yes
Non-contractor (employee)	$A'(a)/C'(a)$	0.39[b]
Non-contractor (employee)	$\Gamma'(D(t,a))$	4.88[a]
Non-contractor (employee)	$a^* \leq a^{sp}$	Yes
Panel B. Monetary loss of one extra hour of temperature exposure exceeding 33°C		
All	Total $ per day	0.77 million
All	$ per day from externality	0.60 million
All	$ per day truck drivers	0.17 million

Notes: This table displays the results of comparing private and social-optimal adaptation levels in Panel A and monetary loss of temperature exposure in Panel B.
[a] Factor of externality, fatality in Table D4.
[b] Our calculation. See Table D5 for parameters and calculating formula.

Table D3: Dangerous Driving Behavior and Crash

	Number of Crash
ln(Number of Dangerous Driving Behaviors)	0.808***
	(0.153)
𝟙[Male]	0.081
	(0.249)
Age	-0.020
	(0.014)
Constant	-4.477***
	(0.836)
Observations	163

Notes: This table reports the estimated coefficients for Equation 2. The data is at the vehicle-driver level. Standard errors in parentheses are clustered at the vehicle level. * $p < 0.1$, ** $p < 0.05$, *** $p < 0.01$.

Table D4: Parameters for Back-of-the-Envelope Calculation

Parameters	Values	Source
Panel A. Estimations		
Effects of extreme temperature on dangerous driving	3%	This paper's estimation
Elasticity of crashes to alarms	0.808	Calibrated using Dingus et al. (2006)
Panel B. Crashes		
Total traffic crashes	155,158	China National Bureau of Statistics
Total fatalities from traffic crash	42,164	China National Bureau of Statistics
Total injuries from traffic crash	142,318	China National Bureau of Statistics
Share of crashes related to trucks	0.28	Beijing Traffic Management Bureau
Factor of externality, fatality	4.88	US, Large Truck and Bus Crash Facts
Factor of externality, injury	2.70	US, Large Truck and Bus Crash Facts
Panel C. Damages		
Property loss from traffic crash	\$1.31 BN	China National Bureau of Statistics
Value of statistical life	\$0.75 MN	Yu (2024)
	\$0.69 MN	Cao et al. (2023)
	\$9.6 MN	US DOT, 2016
Value of injury, severe	\$0.12 MN	Tan et al. (2020)
	\$0.16 MN	US National Safety Council, 2022
Value of injury, minor	\$2,809	Tan et al. (2020)
	\$3,4000	US National Safety Council, 2022

Notes: This table reports parameters related to the back-of-the-envelope calculation. For all parameters, if data from both China and the US are available, we use the data from China in the calculation. If only US data are available, we use that for the calculation. The USD-CNY exchange rate used in the calculation is 7.2. The factor of externality means that for every truck occupant fatality (or injury), the average number of other road users are killed (or injured).

Table D5: Parameters for Cost-Sharing Scheme

Parameters	**Values**	**Source**
Panel A. Estimations		
Total Cost / Total Revenue, (a)	0.5	Survey
Share of Fuel expense in total cost,(b)	0.5	China 2021 Road Freight Industry Key Enterprises Operational Report
Additional fuel cost from AC, (c)	25%	Section 2
lost of revenue from resting, (d)	5%	Figure 4
Cost of AC	6.25%	$a \cdot b \cdot c$
Cost of Resting	3.75%	$\underbrace{[1-a]}_{\text{income w/o. adaptation}} - \underbrace{[(1-ab)(1-d)-a(1-b)]}_{\text{income w. resting}}$

Notes: This table parameters and calculations for the cost-sharing scheme for non-contractors. The loss of revenue from resting is calibrated based on the reduced transportation distance as the result of an additional hour of temperature exposure above 33°C.